Application of Diversity Techniques to WiMAX

by

Srikanth Mettukuru

Problem Report submitted to the
College of Engineering and Mineral Resources
at West Virginia University
in partial fulfillment of the requirements
for the degree of

Master of Science
in
Electrical Engineering

Brian D.Woerner, Ph.D., Chair
Matthew C.Valenti, Ph.D.
Daryl Reynolds, Ph.D.

Lane Department of Computer Science and Electrical Engineering

Morgantown, West Virginia
2007

Keywords: WiMAX, MIMO, OFDM, Space Time Codes, Convolutional Codes,Reed-Solomon codes

Abstract

Application of Diversity Techniques to WiMAX

by

Srikanth Mettukuru
Master of Science in Electrical Engineering

West Virginia University

Brian D.Woerner, Ph.D., Chair

Broadband Wireless Access(BWA) has long held the promise of delivering high speed internet access to business and residential customers and to remote locations where traditional broadband services are unavailable. The publication of a comprehensive industry standard - namely, IEEE 802.16 - representing a distillation of the most advanced technology and an industry consensus permitting equipment interoperability has set the stage for the fulfillment of that promise. IEEE standard 802.16, the first version of which was completed in October 2001 and published on 8 April 2002, defines the Wireless MAN air interface specification for wireless metropolitan area networks (MANs) which are intended to provide high bandwidth wireless voice and data for residential and business customers. Worldwide Interoperability for Microwave Access, commonly known as WiMAX, is an industry consortium that promotes the IEEE 802.16 standard and tests and certifies products for interoperability and compliance with standards. The IEEE 802.16 standard is often referred to as WiMAX today.

The IEEE 802.16a/d standard defines three different PHYs (Physical layers)- WirelessMAN-SCa, WirelessMAN-OFDM and WirelessMAN-OFDMA - to be used in conjunction with the MAC layer to provide reliable end-to-end link. In the present work, the PHY specified for the WirelessMAN-OFDM case is studied and implemented. Various diversity techniques that constitute the PHY to provide a robust system are studied and implemented. Before all of it, firstly, a detailed overview of various broadband access technologies is given in the present work. Then the wireless channel mechanisms are studied and then an overview of the WiMAX PHY's system model is given. Various modulation techniques involved are studied and then each of the performance enhancing techniques are studied one by one with regard to their functionality in the system and the value they add to the system. Finally, simulation results are provided to corroborate the theories deduced.

Acknowledgments

Firstly, I would like to thank Dr.Brian D.Woerner for providing me an opportunity to work with him and for his expert guidance and constant support in completing this work. Then I would like to thank Dr.Matthew C.Valenti for his invaluable suggestions that actually kick started the present work. Special thanks to Dr.Daryl S.Reynolds for being on my committee and for the knowledge he has imparted through his courses. And many thanks to my friends in the Wireless Communications Research Laboratory for providing an ambient atmosphere at the work place and for providing timely cues to complete my work. Finally, I would like to thank all my friends and family members who have been constantly supporting and encouraging me in all my endeavors.

Contents

Acknowledgments **iii**

List of Figures **vi**

List of Tables **viii**

Notation **ix**

1 Introduction **1**
1.1 Broadband - Wired and Wireless . . . 1
1.1.1 Digital Subscriber Line and T-Carrier systems . . . 2
1.1.2 Cable Modem . . . 4
1.1.3 Fiber to the Home and Office . . . 5
1.1.4 Broadband over Powerlines . . . 6
1.1.5 Satellite Broadband . . . 7
1.1.6 Wireless Broadband . . . 8
1.2 Report Outline . . . 10

2 Broadband Wireless Access with Wi-MAX **11**
2.1 The Wireless Channel . . . 11
2.1.1 Large Scale Fading . . . 12
2.1.2 Small Scale Fading . . . 14
2.1.3 Fading Distributions . . . 18
2.2 WiMAX's techniques to combat fading . . . 20
2.2.1 Diversity . . . 20
2.2.2 Adaptive Modulation and Coding rates . . . 23
2.2.3 System Model . . . 24

3 Modulation and Coding in WiMAX systems **25**
3.1 Modulation . . . 25
3.1.1 Phase Shift Keying . . . 27
3.1.2 Quadrature Amplitude Modulation . . . 30
3.1.3 Symbol Mapping . . . 32
3.2 Forward Error Correction . . . 33
3.2.1 Reed-Solomon Codes . . . 34
3.2.2 Convolutional Codes . . . 36

4 Space Time Block Codes and Orthogonal Frequency Division Multiplexing in WiMAX systems **40**
4.1 Space Time Block Codes 40
4.1.1 Bitwise LLR calculations for an STBC system 44
4.2 Orthogonal Frequency Division Multiplexing 47

5 Results and Conclusions **50**
5.1 Results 50
5.1.1 Space Time Block Codes 51
5.1.2 Convolutional codes 51
5.1.3 Reed-Solomon codes 53
5.1.4 OFDM 55
5.2 Conclusion 57

References **59**

List of Figures

2.1 Basic system model 24

3.1 Signal representation on the I-Q axes 27
3.2 Signal constellation diagram for BPSK 28
3.3 Signal constellation diagram for QPSK where the carrier phases are $0, \frac{\pi}{2}, \pi, \frac{3\pi}{2}$ 29
3.4 Signal constellation diagram for QPSK where the carrier phases are $\frac{\pi}{4}, \frac{3\pi}{4}, \frac{5\pi}{4}, \frac{7\pi}{4}$ 30
3.5 Signal constellation diagram for 16-QAM 31
3.6 Signal constellation diagram for 64-QAM 32
3.7 Gray mapping for QPSK, 16-QAM and 64-QAM 33
3.8 A convolutional encoder with memory order m=3 36
3.9 A convolutional encoder with a single input stream 37
3.10 Trellis diagram for the $(5, 7)$ encoder shown in figure 3.9 38
3.11 Convolutional encoder used in the WiMAX PHY 39

4.1 OFDM transmission system 49

5.1 BER performance of the system when QPSK modulation is used and no error reduction techniques are implemented 50
5.2 BER performance of the system when BPSK modulation is used and no error reduction techniques are implemented 51
5.3 BER performance of the BPSK modulated system when Alamouti STBC is implemented 52
5.4 BER performance of the QPSK modulated system when Alamouti STBC is implemented 52
5.5 BER performance of the BPSK modulated system when Convolution coding is added 53
5.6 BER performance of the QPSK modulated system when Convolutional coding is added 53
5.7 BER performance of the BPSK modulated system when concatenated Reed-Solomon-Convolution coding is added 54
5.8 BER performance of the QPSK modulated system when concatenated Reed-Solomon Convolutional coding is added 54
5.9 BER performance of the QPSK modulated system when Reed-Solomon coding is used along with STBC 2Tx-1Rx 55

5.10 BER performance of the QPSK modulated system when Reed-Solomon coding is used along with STBC 2Tx-2Rx 55
5.11 BER performance of the QPSK modulated system when concatenated Reed-Solomon-Convolutional coding is used along with Alamouti STBC 56
5.12 BER performance of the BPSK modulated system when concatenated Reed-Solomon-Convolutional coding is used along with Alamouti STBC 56
5.13 Space-frequency coded OFDM system 57
5.14 BER performance of the BPSK modulated system when concatenated Reed-Solomon-Convolutional coding is used along with the space-frequency coded system 58
5.15 BER performance of the QPSK modulated system when concatenated Reed-Solomon-Convolutional coding is used along with the space-frequency coded system 58

List of Tables

1.1 Upstream and downstream data rates and distance limitations of various forms of Asymmetric DSL. 3
1.2 Upstream and downstream data rates and distance limitations of various forms of Symmetric DSL. 3

2.1 Modulation and coding schemes for 802.16*d*. 23

Notation

We use the following notation and symbols throughout the present work.

$(\cdot)^H$	:	Complex conjugate transpose
$(\cdot)^*$	:	Complex conjugate
$\mathcal{N}_c(0, \sigma^2)$	:	Complex Gaussian distribution with zero mean and variance σ^2 per dimension
$p(x\|y)$	:	Probability of x conditioned on y
$\boldsymbol{I}_K$	:	$K \times K$ Identity matrix
$\Re\{\cdot\}$	:	Real part of the argument

Bold uppercase letters denote matrices while bold lower case letters denote vectors.

Chapter 1

Introduction

'Broadband' can be defined as a type of data transmission in which a wide band of frequencies is available for transmitting information. The availability of a wide band of frequencies enables it to carry multiple data, voice and video channels concurrently. Different channels occupy different frequencies through the transmission medium and empty space in the frequency range between channels ensures that the channels do not interfere with each other.

1.1 Broadband - Wired and Wireless

Various high speed transmission technologies that make up the 'Broadband' picture are:

1. Digital Subscriber Line and T-Carrier Systems
2. Cable Modem
3. Fiber to the Home and Office
4. Powerline Broadband
5. Satellite Broadband
6. Wireless Broadband

Each of these broadband technologies have their pros and cons and a choice among these will depend on a number of factors like the users' location, the minimum speed the user needs, the way the technologies are packaged by the service providers , their pricing etc.

1.1.1 Digital Subscriber Line and T-Carrier systems

Digital Subscriber line (DSL) is a technology that provides digital data transmission over ordinary copper telephone lines. xDSL refers to different variations of DSL such as ADSL, SDSL, HDSL etc. The many versions of DSL come ultimately from one source: telephone companies, who themselves provide DSL services or who lease their lines to other DSL providers.

Twisted pair copper wiring, the kind used by the telephone companies to reach their customers, is capable of handling a much greater bandwidth than that needed for voice. DSL takes advantage of this unused bandwidth to carry extra information over the telephone lines by creating new channels for upstream and downstream traffic. With DSL, digital data need not be converted into analog form and back, unlike a dial-up access where this 'digital-to-analog-to-digital' conversion is needed, which leads to low data rates. This direct transmission of digital signals allows the phone company providing DSL to squeeze in much more information into the telephone line for transmission purposes.

DSL comes in different flavors, which can be broadly classified into two categories: 'Asymmetric DSL' and 'Symmetric DSL'. With Asymmetric DSL, downstream speeds are greater than upstream speeds whereas they are the same for Symmetric DSL. While Asymmetric DSL allows the users to share the line with analog phone, Symmetric DSL doesn't. The various versions of DSL that fall under the Asymmetric DSL category are ADSL, Rate-Adaptive DSL (RADSL), Very High Data Rate DSL (VHDSL/VDSL) and G-Lite. High Data Rate DSL (HDSL), HDSL-2, SDSL and ISDN Digital Subscriber Line (IDSL) constitute the Symmetric DSL category.

DSL suffers from distance limitations. The technology used to implement DSL works over a limited physical distance. At the maximum, DSL runs about 18,000 feet from a telephone exchange. As the distance between the telephone exchange and the user increases, the data

Type	Upstream Speed	Downstream Speed	Maximum Distance
ADSL	16 to 640 Kbps	1.544 to 6.1 Mbps	18,000 feet
RADSL	272 Kbps to 1.088 Mbps	640 Kbps to 2.2 Mbps	25,000 feet
VDSL	1.5 to 2.3 Mbps	13 to 52 Mbps	5,000 feet
G-Lite	512 Kbps	1.544 to 6 Mbps	25,000 feet

Table 1.1: Upstream and downstream data rates and distance limitations of various forms of Asymmetric DSL.

Type	Upstream and Downstream Speed	Maximum Distance
HDSL	1.544 Mbps on two twisted pair lines	12,000 feet
HDSL-2	1.544 to 2.048 Mbps on a single line	18,000 feet
SDSL	1.544 Mbps	12,000 feet
IDSL	128 Kbps	18,000 feet

Table 1.2: Upstream and downstream data rates and distance limitations of various forms of Symmetric DSL.

rates drop down.

Different versions of DSL have different upstream and downstream speed limits and different distance limitations. Tables 1.1 and 1.2 provide [1] some details about the speed and distance limitations of various flavors of Asymmetric DSL and Symmetric DSL respectively.

The T-Carrier system is a digitally multiplexed carrier system that consists of high speed lines made up of multiple channels. A throughput of 64 Kbps can be provided by each channel on a line. A multiplexer combines different channels carrying voice and data into one line so that they can be transmitted at the same time over a single line. The digital signals transmitted over T-carrier systems are PCM-encoded and time-division multiplexed. The T-carrier system uses two pairs of wires and provides full-duplex capability, one pair is used for receiving and another for sending at the same time.

The T-carrier system comes in many forms: T-1, T-2, T-3, T-4 etc, among which T-1 and T-3 are the most popular ones. The T-1 system consists of 24 64-Kbps channels multiplexed and theoretically supports a data rate of 1.544 Mbps. The T-2 system consists of 96 64-Kbps channels multiplexed and theoretically supports a data rate of 6.312 Mbps. The T-3 system consists of 672 64-Kbps channels multiplexed and theoretically supports a data rate of 44.736

[1] from *searchnetworking.com* and [1]

Mbps. Fractional T-1 is a system where only some of the 24 64-Kbps channels are used for the transmission and reception of data.

The telephone companies offer high speed broadband connections through both T-Carrier and DSL systems. While T-1 systems deliver a consistent uninhibited throughput of 1.5 Mbps, DSL systems provide a maximum throughput of 1.5 Mbps. While DSL is handicapped by distance limitations, T-carrier systems are not. But T-carrier systems are expensive because of the robust technology they utilize and become more and more expensive as the user moves to a remote location. T-carrier systems are aimed at businesses for which an always-on high speed internet connection is required while DSL systems are aimed at households and other businesses for which an always-on internet connection is not mission-critical. Nevertheless, Fractional T-1 connections provide an option for people who want to get a better service than DSL, but can't afford the cost of a full T-1 service.

1.1.2 Cable Modem

A cable modem is a device that modulates a data signal over the cable television infrastructure, thus taking advantage of the unused bandwidth on a cable television network to deliver broadband internet. The coaxial cable used to carry cable television can carry hundreds of megahertz of signals whereas each television signal is given only a 6 MHz channel on the cable, thus leaving a lot of bandwidth for data transmission purposes. Data services on cable systems allocate two 6 MHz channels, one for downstream traffic and one for upstream traffic, separated by at least 8 MHz to keep the channels from interfering with each other.

DOCSIS, Data Over Cable Service Interface Specification, is an official standard that defines the interface reqirements for cable modems involved in high speed data distribution over cable television system networks. DOCSIS was developed by Cablelabs, a research consortium that included companies like Cisco, Intel, Motorola, Texas Instruments, Conexant etc.

The speed delivered by a cable modem system depends on the number of users connected to the internet on that cable line at that time since multiple users share a common cable. As the number of users increases, bandwidth available per user decreases and this results

in performance degradation. DOCSIS 3.0 standard details downstream traffic rates between 27Mbps to 36 Mbps and upstream traffic rates between 320 Kbps to 10 Mbps [1]. Unlike a DSL system, the performance of a cable modem doesn't depend on distance from the central cable office.

1.1.3 Fiber to the Home and Office

Fiber to the Home is a broadband telecommunication system based on fiber-optic cables that can deliver multiple services such as high speed internet, telephone and television at the same time. Fiber Optic technology converts electrical signals carrying data to light and sends the light through transparent glass fibers about the diameter of a human hair. Modern fiber optic systems use multiple lasers with different colors to fit multiple signals into the same fiber.

With Fiber to the Home, the fiber is pushed all the way to the individual homes and offices. FTTH is completely free of bandwidth bottlenecks and typically provides for 30 to 100 Mbps service over a coverage area of 33000 feet. Apart from FTTH, there are other fiber optic networks that, together with FTTH, are termed as FTTx networks, which suffer from bandwidth bottle necks due to the use of other broadband technologies such as cable and DSL in conjunction with others. The most common of these architectures are the Fiber to the Building (FTTB), Fiber to the Curb (FTTC) and Fiber to the Node (FTTN) networks. FTTB provides dedicated fiber to each building or block of buildings. The fiber is terminated at a remote terminal from where a cable line or a telephone line connects it to the individual user. FTTB networks provide a speed of 10-100 Mbps when used in conjunction with a cable and a speed of 50Mbps when used in conjunction with DSL over telephone lines. FTTC typically pushes fiber to about 500 to 1000 feet from the subscriber, terminating at a remote terminal and serving about eight to twelve subscribers. In FTTN, the remote terminal is placed at a distance of about 5000 feet from the subscriber and will serve upto 500 subscribers. Both FTTC and FTTN utilize DSL technology to connect to individual users from the remote terminal and provide a rate of about 20 Mbps [2].

[2] numerical data assorted from the internet and [1]

1.1.4 Broadband over Powerlines

Broadband over Power Lines is the use of Power Line Communications technology to provide broadband internet access through utility power lines. Power line communications (PLC) uses RF signals sent over the medium and low voltage AC power lines to allow end users to connect to the internet. The RF signal is modulated by a digital signal and is sent down the power lines in a band of frequencies not used for transmitting electricity. The RF signals travel along the power line wires, pass around the transformers and reach the end user's home or business where an interface converts it into Ethernet compatible data. Most PLC radio signals occupy the frequency band between 1.6 MHz and 80 MHz.

There are three types of Broadband over Power Line (BPL) services: 'In -House BPL', 'Access BPL' and 'Control PLC'. In-House BPL is a home networking technology that uses the transmission standards developed by the HomePlug Alliance to network systems in a home using the electric outlets and the low voltage electric lines in the home. Access BPL uses the medium voltage power lines that are used for local electrical distribution to provide broadband internet access to homes and businesses. Control PLC is used by electric utility companies to control their equipment using the power lines as transmission lines. Functions like Automatic Meter Reading (AMR) and Power grid management can be accomplished using Control PLC.

Power line Broadband supports high data rates up to 45 Mbps in the grid and since it is a shared connection, the actual data rates depend on the number of users serviced per substation. Since power grid is everywhere and most of the infrastructure is already in place, it has become one another promising broadband service option. IEEE P1675 defines the standards for BPL hardware equipment, IEEE P1775 defines the standards for electromagnetic compatibility requirements and testing and measurement methods and IEEE P1901 defines the MAC and PHY layer specifications.

Broadband over Powerline tends to generate much radio interference over the utility line it runs. Most Powerline Communications radio signals occupy the frequency band between 1.6 MHz and 80 MHz and since many shortwave radio broadcasts and amateur radio broadcasts also have their frequency bands in this region, BPL communications tend to interfere with

these already established communications. Since the overhead utility power lines are not shielded and essentially act as antennas, BPL communications also tend to interfere with many unlicensed electronic devices used at homes and businesses [3].

1.1.5 Satellite Broadband

Satellite Broadband is a communication technique where the data is transmitted between the user and the internet service provider through a geosynchronous satellite orbiting the earth over the equator at a distance of about 22,300 miles from the earth's surface. Each user is required to install a satellite dish antenna that points towards the satellite transmitting and receiving the information content.

There are two types of satellite broadband connections: One-way satellite and Two-way satellite. In One-way satellite systems, a dial-up modem is also used in addition to a satellite modem. The downstream traffic from the ISP to the end-user is transmitted through the satellite whereas the upstream traffic from the user to the ISP is transmitted through a normal dial-up connection. A Two-way satellite system, as the name suggests, uses the satellite for upstream and downstream traffic. While a one-way satellite system necessitates the use of a dedicated dial-up connection for an always on internet connection, the two-way system requires a more complicated and expensive satellite dish that has the ability to transmit an upstream signal 22,300 miles into the air to reach the satellite.

Satellite Internet systems are handicapped by latency, the time data takes to travel from the sender to the receiver. In a two-way satellite system, a single transaction requires the electromagnetic signals to make two round-trips between the earth's surface and the actual satellite which is orbiting 22,300 miles above the equator. One round-trip is between the user's satellite dish antenna and the satellite, the other round trip is between the satellite and the internet service provider's satellite system hub. Such an arrangement inherently produces transmission delay due to the large distances involved and this delay, in addition to the network delays caused by the land-based data transfer between the ISP and the accessed web server, makes the satellite internet system a bad choice for interactive applications like

[3] numerical data assorted from the internet and [1]

online gaming and Voice over IP. Further, satellite internet systems are adversely affected by inclement weather conditions as all other satellite links.

Since satellite internet systems are shared bandwidth systems, the speed depends on the amount of internet traffic also, apart from the latency. The typical speeds a consumer can expect to get are a download speed of about 500 Kbps and an upload speed of about 80 Kbps. Since these speeds are lesser than the ones other forms of broadband services provide, satellite internet tends to occupy mostly the rural areas which are deprived of other forms of broadband services. Satellite broadband is expensive in comparison to other broadband services since building a satellite and the customer equipment is expensive and these expenses accrue to the subscribers [4].

1.1.6 Wireless Broadband

Wi-Fi is a generic term used to represent wireless local area networks (WLAN) that comply with the IEEE 802.11 wireless networking standards. IEEE 802.11 specifies an over-the-air interface between a wireless client and a base station or between two wireless clients.

IEEE 802.11 comes in many versions: 802.11a, 802.11b, 802.11g and 802.11n etc, all of which operate in the unlicensed frequency bands. 802.11a operates in the 5 GHz frequency band using the 'Orthogonal Frequency Division Multiplexing (OFDM)' technology and provides a data rate of 54 Mbps. 802.11b operates in the 2.4 GHz frequency band using the 'Direct Sequence Spread Spectrum (DSSS)' technique and provides a data rate of 11 Mbps. 802.11g operates in the 2.4 GHz frequency band using the OFDM technology and provides a data rate of 54 Mbps. OFDM increases bandwidth and data capacity by splitting a broad carrier channel into multiple, closely spaced narrowband carriers, each of which use a different frequency to transmit different parts of a message. Also the narrowband carriers are placed such that neighboring carrier channels are orthogonal to one another to avoid overlap and thereby interference. 802.11n is expected to deliver a typical data rate of about 200 Mbps over a wider range using the 'Multiple Input Multiple Output (MIMO)' technique in addition to the OFDM technology. MIMO uses multiple transmit and receive antennas to

[4] numerical data assorted from the internet and [1]

increase the data throughput and reliability of a wireless communication system.

Wi-Fi obviates the necessity of cables to set up a LAN and is most useful for providing wireless broadband access within offices and households, when paired in conjunction with other standard broadband access techniques. But Wi-Fi is distance-limited. A Wi-Fi hotspot can deliver broadband internet access to clients within a distance range of about 100 meters from it. Although newer technologies using directional antennas and mesh-networks with Wi-Fi increase the distance range of a Wi-Fi hotspot to more than 100 meters, they do not provide a standardized way of connecting Wireless Internet Service Providers (WISPs) directly to homes and offices. This problem is widely known as the 'last mile' problem.

WiMAX, short for 'Worldwide Interoperability for Microwave Access', is an effective 'last mile' solution for delivering broadband directly to homes and offices by the WISPs. The WiMAX technology is based on the IEEE 802.16 standard which in turn defines the WirelessMAN air interface specification for wireless metropolitan area networks.

The original standard, IEEE 802.16, specified WiMAX in the 10 to 66 GHz range for *line of sight* (LOS) operation. Later, IEEE 802.16a was developed for use in licensed and license-exempt frequencies from 2 to 11 GHz for *non line of sight* (NLOS) operation. The IEEE 802.16d, also known as the IEEE 802.16-2004, is an update to the IEEE 802.16a and is a 'fixed' broadband access solution for the last mile. This standard is referred to as a 'fixed' solution because it uses a mounted antenna at the subscriber's site. The IEEE 802.16e standard, also called 'mobile WiMAX', is an amendment to the 802.16d specification and adds 'portability' to the standard. While 'fixed WiMAX' applications are point-to-multipoint enabling broadband access to homes and businesses, 'mobile WiMAX' offers the full mobility of cellular networks at true broadband speeds.

WiMAX operates both in the licensed spectrum and the unlicensed spectrum. WiMAX has a long transmission range of about 30 miles because of its inherent use of directional antennas. While 802.16 can deliver a maximum throughput rate of about 124 Mbps, 802.16a can deliver a throughput rate of only 70 Mbps since it has to encounter the NLOS conditions in the 2-11 GHz range. While Wi-Fi uses a 64-carrier OFDM scheme, WiMAX uses a 256-carrier OFDM scheme, enabling it to deliver a high data rate. The mobile version of WiMAX, 802.16e, uses Orthogonal Frequency Division Multiple Access (OFDMA), which

not only divides the carriers into multiple subcarriers as in OFDM, but also groups those multiple subcarriers into sub-channels. WiMAX also relies upon a grant-request access protocol which, in contrast to the contention-based access used under Wi-Fi, doesn't allow data collisions and, therefore, uses the available bandwidth more efficiently. Both 'fixed WiMAX' and 'mobile WiMAX' have flexible channel bandwidths between 1.5 and 20 MHz to facilitate transmission over longer ranges and to different types of subscriber platforms [5].

1.2 Report Outline

The present report continues as follows. In Chapter 2, the wireless channel and its large and small scale fading mechanisms and various fading distributions are discussed. Then various techniques used by WiMAX to combat the fading conditions of the channel are briefly discussed. Finally, the system model used in the present work is described. Chapter 3 starts with an overview of the modulation techniques used in the system. Then it delves into the details of the time diversity techniques used in the system, namely forward error correction techniques. It presents an overview of the Reed-Solomon codes and Convolutional codes which are used in the present work. Chapter 4 describes various other diversity techniques used in the system such as the Space Time Block Codes (STBC) and the Orthogonal Frequency Division Multiplexing (OFDM). Further, calculation of the bitwise loglikelihood ratios (LLR) for an Alamouti STBC scheme is explained in a detailed manner. Chapter 5 showcases the results of the present work before wrapping it up with some concluding remarks.

[5] numerical data assorted from the internet and [1]

Chapter 2

Broadband Wireless Access with Wi-MAX

2.1 The Wireless Channel

An ideal channel model called the additive-white-Gaussian-noise (AWGN) channel is the usual starting point in analyzing the performance of a wireless communication system. In this model,the transmitted data samples are corrupted by a set of statistically independent noise samples where the noise samples are produced by the thermal noise generated at the receiver. Thermal noise is produced by the random movement of electrons due to thermal agitation in a receiver. The term *Gaussian* is used to denote that this thermal noise has a Gaussian distribution. The current introduced by the random movement of electrons can be regarded as the sum of many individual small currents produced by a very large number of electrons and since all these current sources behave independently, the total current is considered to be the sum of a large number of independent and identically distributed (i.i.d) random variables. By applying the central limit theorem which says that the distribution of the sum of a large number of i.i.d random variables approaches a Gaussian distribution, this total current has a Gaussian behavior. The term *white* is used to indicate that this noise has equal power over all the frequency components, i.e. the power spectral density is constant for all frequencies and is equal to $\frac{N_0}{2}$, where $\frac{N_0}{2}$ is called the two-sided noise spectral density. The term *additive* implies that the noise samples are added to the transmitted data samples

thereby corrupting them. Thus the complex-valued received signal under the AWGN channel is given by

$$r(t) = s(t) + n(t) \tag{2.1}$$

where *s(t)* is the transmitted signal and *n(t)* is the noise signal whose samples have a mean of 0 and a variance of $\frac{N_0}{2}$.

Unfortunately, the AWGN model is not appropriate for wireless channels because the transmitted signal is also subject to the 'fading' phenomenon introduced by the wireless channels, in addition to the noise introduced by the receiver. *Fading* represents the fluctuations in the instantaneous received signal strength due to the multitude of propagation paths traversed by the signal. The signal gets reflected by various objects in its path as it travels from the transmitter to the receiver, thus travelling through multiple paths to the receiver. These multipath components add constructively or destructively at the receiver depending upon their attenuation factors and phase angles thus causing the received signal strength to fluctuate with time and distance. The basic mechanisms that affect a signal propagating in a wireless medium are Reflection, Diffraction and Scattering [2]. *Reflection* occurs when the propagating signal bounces off an object with dimensions relatively larger than the wavelength of the signal. *Diffraction* occurs when the propagation path between the transmitter and receiver is obstructed by a dense body with dimensions that are relatively larger than the wavelength of the signal, causing secondary waves to be formed behind the obstructing body. *Scattering* occurs when the propagating signal strikes an object whose dimensions are on the order of the wavelength of the signal or less thereby spreading out the signal energy in all directions. These three basic propagation mechanisms together result in two types of fading largely described as *Large Scale Fading* and *Small Scale Fading*.

2.1.1 Large Scale Fading

Large scale fading represents the average signal power attenuation or the path loss due to motion over large areas. *Path Loss* and *Shadowing* are the two basic mechanisms that constitute the large scale fading effects.

Path Loss

Path Loss is best described by the *free space path loss* model. In the free space path loss model, it is assumed that the transmitting antenna is isotropic, i.e., the transmitter radiates energy with equal intensity in all directions and that there are no objects in the propagation path between the transmitter and the receiver to block the signal or create its reflections. It is also assumed that the transmission medium does not absorb energy [3]. The power received by a receiving antenna in the free space model is given by the *Friis free space* equation as [2]:

$$P_r(d) = \frac{P_t G_t G_r \lambda^2}{(4\pi d)^2 L} \tag{2.2}$$

where P_t is the transmitted power, $P_r(d)$ is the received power which is a function of the distance between the transmitter and the receiver, G_t is the gain of the transmit antenna, G_r is the gain of the receive antenna, λ is the wavelength of the signal, d is the distance between the transmitter and the receiver and L is the system loss factor not related to propagation. It can be observed that the received signal power is inversely proportional to the square of the distance between the transmit and receive antennas. Hence, as the distance between the transmitter and the receiver increases, the received signal power decreases. Equation 2.2 can be written as

$$P_r(d) = \left(\frac{P_t G_t G_r \lambda^2}{(4\pi d_0)^2 L}\right)\left(\frac{d_0}{d}\right)^2 \tag{2.3}$$

where d_0 is the reference distance in the far field of the antenna. The free space path loss *PL(d)* is the signal attenuation between the transmit and receive antennas and is given as [4]:

$$PL(d) = \frac{P_t}{P_r(d)} \tag{2.4}$$

$$= \left(\frac{(4\pi d_0)^2 L}{G_t G_r \lambda^2}\right)\left(\frac{d}{d_0}\right)^2 \tag{2.5}$$

In decibels, the above equation can be written as

$$PL(d)_{dB} = PL(d_0)_{dB} + 20\log_{10}\left(\frac{d}{d_0}\right) \tag{2.6}$$

$$= PL(d_0)_{dB} + (10)(2)\log_{10}\left(\frac{d}{d_0}\right) \tag{2.7}$$

In general, the above equation can be written as

$$\overline{PL}(d)_{dB} = PL(d_0)_{dB} + 10n \log_{10}\left(\frac{d}{d_0}\right) \tag{2.8}$$

where n is called the 'path loss exponent' and is equal to 2 for free space and greater than 2 for practical channels.

Shadowing

Shadowing refers to the variations in the received signal power over large distances due to the random effects of the terrain and objects in the environment. It is the reason why two different receivers equidistant from the transmitter receive the transmitted signal at different powers. Shadowing is modelled as an additional random component added to the path loss and thus the effective path loss at a particular distance from the transmitter is random and is said to be log-normally distributed about its mean value $\overline{PL}(d)$. This form of shadowing is called *log-normal shadowing* and it can be modelled as [2]:

$$\begin{aligned} PL(d)_{dB} &= \overline{PL}(d)_{dB} + X_\sigma \,\text{dB} && (2.9)\\ &= PL(d_0) + 10n \log_{10}\left(\frac{d}{d_0}\right) + X_\sigma && (2.10) \end{aligned}$$

where $X_\sigma \sim \mathcal{N}(0, \sigma^2)$,i.e.,$X_\sigma$ is a Gaussian random variable with mean 0 and variance σ^2.

2.1.2 Small Scale Fading

Small scale fading refers to the rapid fluctuations in the received signal power over a short period of time or travel distance, where large scale effects may be ignored, as the mobile units move from one place to another. This type of fading occurs when two or more versions of a transmitted signal arrive at the receiver with different propagation delays, amplitudes, phases and angles of arrival. Since the multiple versions of the transmitted signal traverse along different paths, these are often called multipath components and they combine constructively or destructively causing fading.

A mobile radio channel can be accurately modelled as a linear time-variant filter and its impulse response completely characterizes a multipath fading channel [4]. The impulse

response of such a channel is given by

$$h(\tau;t) = \sum_{n=1}^{N} \alpha_n(t) e^{-j2\pi f_c \tau_n(t)} \delta(\tau - \tau_n(t)) \tag{2.11}$$

where f_c is the carrier frequency, N is the number of paths, $\alpha_n(t)$ and $\tau_n(t)$ are the complex attenuation factor and propagation delay of the n-th path respectively. The transfer function of the time-variant channel is the Fourier transform of the time-variant impulse response and is given by

$$H(f;t) = \int_{\infty}^{-\infty} h(\tau;t) e^{-j2\pi f\tau} d\tau \tag{2.12}$$

Variations in $H(f;t)$ as f varies causes time-spreading of the underlying digital pulses within the signal and this behavior of the channel is called 'time-dispersive' or 'frequency-variant' nature of the channel. Similarly, variations in $H(f;t)$ as t varies causes spreading in the frequency domain and this behavior of the channel is called 'frequency-dispersive' or 'time-variant' nature of the channel. Delay time τ in (2.12) refers to the time-spreading manifestation which results from the fading channel's non-optimum impulse response whereas the observation time t refers to the time-varying nature of the channel caused by relative motion between a transmitter and receiver, or by movement of objects within the channel [5]. Either of the two small-scale fading mechanisms can be equivalently studied in both time-domain and frequency-domain. Bello in [6] proposed the notion of Wide-Sense Stationary Uncorrelated Scattering (WSSUS) to study the small-scale fading phenomenon. The WSSUS assumption allows the general autocorrelation of the transfer function to be written as

$$\phi_H(\triangle f; \triangle t) = E\left[H^*(f;t) H(f + \triangle f; t + \triangle t)\right]. \tag{2.13}$$

The function $\phi_H(\triangle f; \triangle t)$ is called as *spaced-frequency, spaced-time correlation function* of the channel.

Time Dispersive Channel

If the channel is assumed to be time-invariant, then the spaced-frequency, spaced-time correlation function $\phi_H(\triangle f; \triangle t)$ can be written as

$$\phi_H(\triangle f; \triangle t) = \phi_H(\triangle f) \tag{2.14}$$

$\phi_H(\triangle f)$ is called the *spaced-frequency correlation function* of the channel and it represents the correlation between the channel's response to two signals as a function of the frequency difference between the two signals. It can also be thought of as the channel's frequency transfer function. The width over which $\phi_H(\triangle f)$ is non-zero is called the *coherence bandwidth*(B_m) of the channel and it is a statistical measure of the range of frequencies over which the channel passes all the spectral components with approximately equal gain and linear phase. If the bandwidth of the transmitted signal (B_s) is less than the coherence bandwidth of the channel, all the individual frequency components of the transmitted signal undergo the same amount of fading, i.e., $H(f;t)$ is constant in the f variable and the signal is said to undergo *flat fading*. If the bandwidth of the transmitted signal is greater than the coherence bandwidth of the channel, different frequency components of the transmitted signal undergo different fading attenuations and delays, i.e., $H(f;t)$ is not constant in the f variable, and the signal is said to undergo *frequency selective fading*.

A completely analogous characterization of signal dispersion can be made in the time domain. The *multipath intensity profile* (or *power delay profile*) is the inverse Fourier Transform of the spaced-frequency correlation function and is given as

$$\phi_h(\tau) = F^{-1}\{\phi_H(\triangle f)\} \tag{2.15}$$

The multipath intensity profile provides information on how the average received power varies as a function of time delay τ for a transmitted signal. The width over which $\phi_h(\tau)$ is non-zero is called the *maximum excess delay* (T_m) and it is the time interval between the first and last received components of a transmitted impulse during which the multipath signal power falls to some threshold level below that of the strongest component. The maximum excess delay and the coherence bandwidth are reciprocally related, i.e., $T_m \approx \frac{1}{B_m}$. A channel is said to exhibit *flat fading* when the maximum excess delay is less than the symbol duration (T_s) in which case all the received multipath components of a symbol arrive within the symbol duration, thereby making the components unresolvable. A channel is said to exhibit *frequency selective fading* when the maximum excess delay is greater than the symbol duration (T_s). Frequency selective fading results in the received signal having multiple randomly delayed and attenuated versions of the transmitted signal and this results in the received multipath

components of a symbol extend beyond the symbol's time duration. Thus the delayed versions of a previously transmitted symbol interfere with the present transmitted symbol and this results in channel-induced *intersymbol interference*.

Time Variant Channel

If the channel is assumed to be time variant and not time dispersive, then the spaced-frequency, spaced-time correlation function $\phi_H(\triangle f; \triangle t)$ can be written as

$$\phi_H(\triangle f; \triangle t) = \phi_H(\triangle t) \tag{2.16}$$

$\phi_H(\triangle t)$ is called the *spaced-time correlation function* of the channel and it specifies the extent to which there is correlation between the channel's responses to two similar signals sent at different time instances. The *coherence time* (T_0) of a channel is a measure of the time duration over which the channel's response is essentially invariant or behaves in a correlated manner. If T_0 is less than the transmitted symbol duration (T_s), then the fading character of the channel will change several times while a symbol is propagating, leading to its distortion. This type of fading is called *fast fading*. If T_0 is greater than the transmitted symbol duration (T_s), then the channel remains virtually unchanged during the symbol transmission time and no distortion of the symbol takes place. This type of fading is called *slow fading*.

Analogously, the frequency domain or the Doppler shift domain can also be used to completely describe the time-variant nature of the channel. The Fourier Transform of the spaced-time correlation function ($\phi_H(\triangle t)$) is called the *Doppler Power Spectrum* $S_H(\lambda)$.

$$S_H(\lambda) = F\{\phi_H(\triangle t)\} \tag{2.17}$$

The Doppler Power Spectrum of the channel gives the signal power as a function of the Doppler-frequency shift (λ) and yields information about the spectral spreading of a transmitted signal in the frequency domain. The width over which the Doppler Power Spectrum of a channel is non-zero is called the *Doppler spread* or *spectral broadening*(B_d) of the channel and it is reciprocally related to the coherence time of the channel ,i.e., $B_d \approx \frac{1}{T_0}$. The Doppler spread is also regarded as the *fading bandwidth* or *fading rate* of the channel. If the Doppler spread or fading bandwidth (B_d) of the channel is greater than the bandwidth of

the transmitted signal (B_s), then the channel is said to be *fast fading* and it is said to be *slow fading* if the fading bandwidth is less than the transmitted signal bandwidth.

The Spaced-frequency correlation function and the Spaced-time correlation function are considered to be a pair of dual functions since they exhibit similar behavior across domains [5]. Similarly, Multipath intensity profile and Doppler power spectrum are also considered to be dual functions.

2.1.3 Fading Distributions

Fading parameters such as the attenuation and delay are usually modelled as random processes since they cannot be known deterministically. The delays are often considered to be uniformly distributed over a reasonable number of symbol periods [4]. The envelope of the received signal, which depends on the attenuation, is modelled by different probability distributions according to the presence or non-presence of *Line of Sight* (LOS) path between the transmitter and the receiver and the severity of the fading channel conditions. Most of these models assume a large number of scatterers so that the central limit theorem can be used to model the channel.

Rayleigh Fading

The Rayleigh fading model is used for channels that do not have a strong line of sight signal component between the transmitter and the receiver. The fading coefficient is written as

$$\alpha(t)e^{-j2\pi f_c \tau(t)} = x(t) + jy(t) \tag{2.18}$$

where $x(t)$ and $y(t)$ are said to be independent real Gaussian random processes. The notion of Gaussian comes from the fact that a large number of scatterers are assumed and the application of the central limit theorem to these random scatterers yields a Gaussian distribution. $x(t)$ and $y(t)$ are also said to be zero mean because of the absence of a strong line of sight signal component. Mathematically, if we have two independent and identically distributed Gaussian random variables X and Y with mean 0 and variance σ^2, then R = $\sqrt{X^2 + Y^2}$ has

a Rayleigh distribution with the probability density function given by:

$$p_R(r) = \begin{cases} \frac{r}{\sigma^2} \exp\left[\frac{-r^2}{2\sigma^2}\right] & \text{for } r \geq 0 \\ 0 & \text{otherwise.} \end{cases} \tag{2.19}$$

Nakagami-*m* Fading

The envelope of the received signal can be modelled by a more general, statistical model called the Nakagami-m distribution, whose probability density function is given by

$$p_X(x) = \frac{2}{\Gamma(m)} \left(\frac{m}{2\sigma^2}\right)^m x^{2m-1} e^{\frac{-mx^2}{2\sigma^2}} \tag{2.20}$$

where $\Gamma(m) \triangleq \int_0^\infty t^{m-1}e^{-t}dt$. The Nakagami-$m$ distribution reduces to the Rayleigh distribution when $m = 1$. The parameter m can be tuned to match the degree of the severity of the fading channel conditions.

Rician Fading

The Rician fading model is used for channels that have a strong line of sight signal component between the transmitter and the receiver. The fading process can be written as

$$\alpha(t)e^{-j2\pi f_c \tau(t)} = x(t) + jy(t) + a_0 \tag{2.21}$$

where a_0 is a constant that represents the amplitude of the line of sight component. The strength of the line of sight component is defined by the Rice factor $K = \frac{a_0^2}{2\sigma^2}$. The Rician distribution degenerates to a Rayleigh distribution when the dominant line of sight component fades away, i.e., when a_0 becomes equal to 0.

In summary, path loss, shadowing and multipath fading are the three main concerns to be addressed when a wireless channel is used as the transmission medium, among which only multipath fading is addressed in this work. The Rayleigh fading model is used to model the wireless channel in this work, where every transmitted symbol encounters a different fading coefficient as it travels to the receiver. The channel also adds AWGN noise to the transmitted symbol. With this kind of model, the received symbol r can be written as

$$r = hs + n \tag{2.22}$$

where h is the complex Rayleigh fading coefficient, s is the transmitted symbol and $n \sim \mathcal{N}_c(0, \sigma^2)$ is the complex additive-white-Gaussian-noise.

2.2 WiMAX's techniques to combat fading

To mitigate the effects of *fading* and *intersymbol interference* when WiMAX is used in the 2-11 GHz range for *non line of sight* (NLOS) operation, various techniques have been introduced into the Physical layer (PHY) of the WiMAX system. The following sections give an overview of some of those techniques.

2.2.1 Diversity

Diversity is a powerful communication technique that combats fading by exploiting the random nature of the wireless channel and finding independent (highly uncorrelated) signal paths between the transmitter and the receiver. Even if some of those signal paths undergo a deep fade, other independent paths may have a strong signal and by having more than one path to choose from, a considerable increase in the level of performance can be achieved [2]. The three main forms of diversity used by the WiMAX PHY are *Time Diversity*, *Frequency Diversity* and *Spatial Diversity*.

Time Diversity

Time Diversity is achieved by repeatedly transmitting the same signal in different time slots, where the separation between the successive time slots equals or exceeds the coherence time of the channel. If the channel is time varying, each copy will experience different channel conditions and this results in the reception of multiple, independently faded copies of the transmitted signal at the receiver, thereby providing for diversity. Channel coding techniques such as the Convolutional codes, Turbo codes, Reed-Solomon codes etc and RAKE receiver for spread spectrum CDMA are considered as time diversity techniques. The WiMAX system takes advantage of time diversity by incorporating an outer Reed-Solomon block code concatenated with an inner convolutional code into its physical layer. Turbo coding has been left as an optional feature, which can improve the coverage and/or capacity of the system, at

the price of increased decoding latency and complexity. In the present work, only an outer Reed-Solomon code concatenated with an inner convolutional code is used. Further details of the Reed-Solomon code and the convolutional code used are included in chapter 3.

Frequency Diversity

Frequency diversity is achieved by transmitting the same information bearing signal on different carrier frequencies, where the separation between successive carriers equals or exceeds the coherence bandwidth of the channel. If the channel is frequency selective, each copy may experience different channel conditions and this results in the reception of multiple copies that can be manifested as resolvable multipath in frequency selective fading channels, thereby providing for diversity. *Spread Spectrum Modulation* and *Orthogonal Frequency Division Multiplexing* (OFDM) are considered as frequency diversity techniques. In Spread Spectrum Modulation, if the coherence bandwidth of the channel is more than the signal bandwidth, the signal's bandwidth is increased to create frequency selectivity. OFDM exploits frequency diversity by providing simultaneous modulation signals with error control coding across a large bandwidth, so that if a particular frequency undergoes a fade, the composite signal will still be demodulated [2].

Apart from providing a PHY with a single-carrier modulated air interface (WirelessMAN-SCa), the IEEE 802.16a/d standard also defines two other PHYs which use the OFDM scheme [7].

1. WirelessMAN-OFDM is a 256-carrier OFDM scheme where multiple access of different subscriber stations is time-division multiple access (TDMA) based.

2. WirelesMAN-OFDMA is a 2048-carrier OFDM scheme where multiple access of different subscriber stations is provided using a combination of TDMA and OFDMA.

The two OFDM-based systems are more suitable for non-LOS operation because the equalization process is more simpler for multicarrier signals. Of the two, the 256-carrier version has been specified by all the system profiles currently defined by the WiMAX Forum, which is a consortium of all the organizations promoting WiMAX. For this reason, the 256-carrier

OFDM scheme is considered in this work along with the single carrier scheme. Chapter 4 further explains this topic.

Spatial Diversity

Spatial Diversity, also called *Antenna Diversity*, is achieved by having multiple antennas at the transmitter or the receiver or both at the transmitter and the receiver (*Multiple Input Multiple Output*(MIMO) communications). Separation on the order of a few wavelengths is required between two antennas in order to obtain independently faded signals [8] which provide for diversity. In a system with m transmit antennas and n receive antennas, the maximal diversity gain is mn when the fading coefficients between individual antenna pairs are assumed to be independent, identically distributed (i.i.d.) Rayleigh faded [9].

Space Time Coding techniques such as *Space Time Block Codes* (STBC) and *Space Time Trellis Codes* (STTC) target on achieving high diversity gains. Apart from achieving diversity gain, Space Time Trellis codes achieve coding gain also, but the decoding complexity of STTC is much higher compared to that of the STBC. While space-time coding techniques improve the reliability of reception, there are other MIMO techniques that increase the rate of communication for a fixed reliability level by increasing the *degrees of freedom* available for communication [10][11]. One such technique is the *Bell Labs Space Time Architecture* BLAST system which achieves multiplexing gain by transmitting independent symbol streams from multiple transmit antennas. When the paths between individual transmit-receive antenna pairs fade independently, multiple spatial parallel channels are created and by transmitting independent information streams through these spatial channels, the data rate can be increased. This effect is also called *spatial multiplexing* [12]. Thus, while the goal of the BLAST system is to achieve multiplexing gain by transmitting M symbols/channel use, where M is the number of transmit antennas, the Space Time Coding techniques try to achieve maximum diversity gain and transmit 1 reliable symbol/channel use. The spectral efficiency of the Space time coding schemes can be improved by using modulation techniques that have higher modulation order, but this leads to a degraded error performance as higher constellations have their signals close to each other. Thus there exists a fundamental tradeoff between diversity and multiplexing gains in a point-to-point wireless fading channel that sets

Modulation	Coding Rate
BPSK	1/2
QPSK	1/2
QPSK	3/4
16QAM	1/2
16QAM	3/4
64QAM	2/3
64QAM	3/4

Table 2.1: Modulation and coding schemes for 802.16*d*.

a limit on the overall performance of a MIMO system.

The WiMAX PHY designates Space-time block codes as an optional feature that can be implemented in the downlink to provide increased diversity [7]. A 2×1 or 2×2 Alamouti STBC [13] scheme may be implemented which provides both time diversity and space diversity. The present work implements both the schemes to highlight the advantage of using receive diversity as well, since receive diversity needs no additional transmit power. Alamouti STBC schemes and their implementation in the present work are further explained in chapter 4.

2.2.2 Adaptive Modulation and Coding rates

The 802.16a/d standard defines seven combinations of modulation and coding rate that can be used to achieve various trade-offs of data rate and reliability, depending on the severity of the channel's fading conditions. These possible combinations are shown in Table 2.1. Using a modulation with higher modulation order increases the data rate, but degrades the reliability of the system and viceversa. A rate 1/2 Convolutional encoder is used in the WiMAX PHY and by using *puncturing*, an overall code rates of 2/3 and 3/4 can be achieved. Puncturing is the process of removing some of the parity bits after encoding. In the present work, only BPSK and QPSK modulation schemes are used and no puncturing is performed, i.e., the code rate of the inner convolutional code is set to 1/2 constantly.

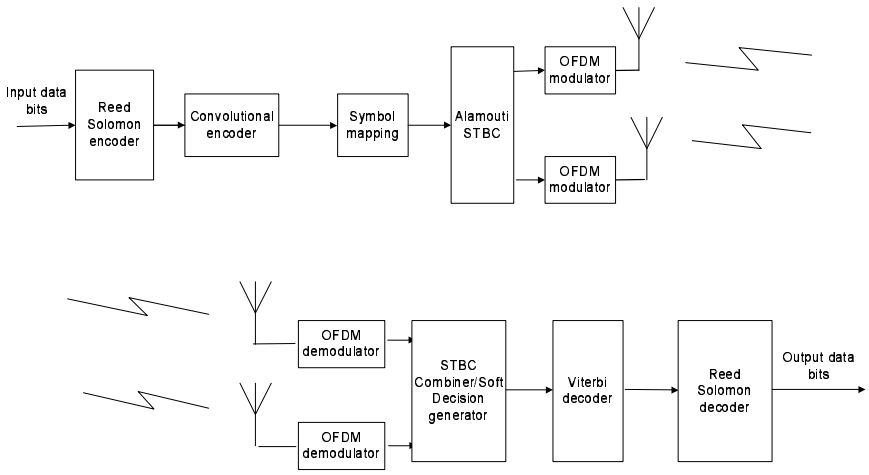

Figure 2.1: Basic system model

2.2.3 System Model

Figure 2.1 shows the basic system model of the WiMAX PHY that is simulated in this work. The *Bit Error Rate* (BER) performance of the system is simulated and the variation in performance, as different diversity techniques are introduced, is noticed.

Chapter 3

Modulation and Coding in WiMAX systems

3.1 Modulation

Modulation is the process by which digital symbols are mapped onto analog waveforms that are compatible with the characteristics of the channel. It generally involves translating a baseband message signal to a bandpass signal at frequencies that are very high when compared to the baseband frequency. The bandpass signal is called the *modulated signal* and the baseband message signal is called the *modulating signal*. Modulation translates a low pass message signal to a bandpass signal and this is required since transmitting a low pass signal would require huge antennas and also since the low frequency band is home to many natural and man-made noise sources [4].

A bandpass signal can be represented in the form

$$s(t) = x(t)\cos(2\pi f_c t) - y(t)\sin(2\pi f_c t) \tag{3.1}$$

where $x(t)$ and $y(t)$ are real-valued low-pass signals called the *in-phase* and *quadrature* components of $s(t)$ and this form of representation is called the *Quadrature* notation. Another notation that can be used to represent a bandpass signal is the *Magnitude and Phase* notation which represents a bandpass signal as

$$s(t) = a(t)\cos(2\pi f_c t + \Theta(t)) \tag{3.2}$$

where $a(t)$ is the *amplitude* and $\Theta(t)$ is the *phase* of $s(t)$. Modulated signals carry information by varying any of the three parameters - amplitude, phase, and frequency of the bandpass signal. Amplitude Shift Keying(ASK) carries information by varying the amplitude $a(t)$ of the bandpass signal according to the message signal. Phase Shift Keying(PSK) varies the phase $\Theta(t)$ of the bandpass signal whereas Frequency Shift Keying(FSK) varies the instantaneous frequency at which the bandpass signal is centered about. Quadrature Amplitude Modulation(QAM) is a combination of ASK and PSK where both amplitude and phase of the bandpass signal are varied according to the message signal. Since WiMAX uses different forms of PSK and QAM, we will concentrate only on them in this work.

In digital modulation, $x(t)$ and $y(t)$ in equation 3.1 vary according to the signal chosen to be transmitted from a fixed set of M possible signals that are known both to the transmitter and the receiver. Typically, $M = 2^R$ where $R \geq 1$ is the number of bits assigned to each signal in the signal set. Thus $\log_2 M$ bits are transmitted every time a signal from the signal set is transmitted. The m-th signal in the signal set can be written as [4]

$$s_m(t) = x_{r,m}\phi_1(t) + x_{i,m}\phi_2(t),\ 0 \leq t \leq T_s,\ m = 1, 2, ...M \tag{3.3}$$

where

$$\phi_1(t) = \sqrt{\frac{2}{T_s}} g(t) \cos 2\pi f_c t \tag{3.4}$$

$$\phi_2(t) = -\sqrt{\frac{2}{T_s}} g(t) \sin 2\pi f_c t \tag{3.5}$$

$x_{r,m}, x_{i,m} \in \mathbb{R}$, and $g(t)$ is a bandwidth and time limited pulse known to the transmitter and the receiver. The scale factor $\sqrt{\frac{2}{T_s}}$ and $g(t)$ are chosen to ensure that $\phi_1(t)$ and $\phi_2(t)$ are orthonormal so that they span the signal space and $(x_{r,m}, x_{i,m})$ are the coordinates of each signal in the signal space. Here $\phi_1(t)$ is said to be the in-phase(I) axis and $\phi_2(t)$ is said to be the quadrature(Q) axis of the signal constellation diagram in which a signal is shown by its projections onto the in-phase and quadrature axes as shown in figure 3.1. The points in the constellation are called *symbols* and are given by $s_m = x_{r,m} + jx_{i,m}$ $(1 \leq m \leq M)$.

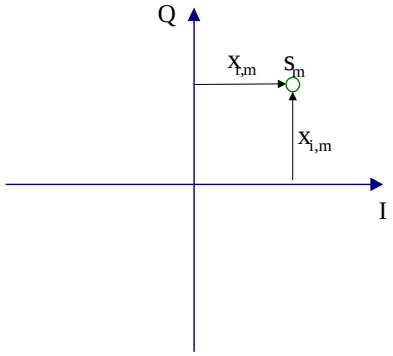

Figure 3.1: Signal representation on the I-Q axes

3.1.1 Phase Shift Keying

In Phase Shift Keying, the phase of a constant amplitude carrier signal is switched between distinct phases in accordance with the message bits. M-ary PSK signals can be obtained by putting

$$x_{r,m} = \sqrt{E_s}\cos\left[\frac{2\pi}{M}(m-1)\right] \tag{3.6}$$

$$x_{i,m} = \sqrt{E_s}\sin\left[\frac{2\pi}{M}(m-1)\right] \tag{3.7}$$

into equation 3.3, where E_s is the *symbol energy*, i.e., the transmitted signal energy per symbol.

Binary Phase Shift Keying

Binary Phase Shift Keying (BPSK) involves the transmission of two different signals for a binary 1 and a binary 0. The phase the carrier signal is switched between 0 and π radians according to the two baseband signals corresponding to binary 1 and 0. The two signals in the signal set for BPSK modulation can be obtained by putting $M = 2$ into equations 3.3, 3.6 and 3.7. Thus we obtain

$$s_1(t) = \sqrt{E_s}\phi_1(t) \tag{3.8}$$

$$= \sqrt{\frac{2E_s}{T_s}}g(t)\cos 2\pi f_c t \tag{3.9}$$

$$s_2(t) = -\sqrt{E_s}\phi_1(t) \tag{3.10}$$

$$= -\sqrt{\frac{2E_s}{T_s}}g(t)\cos 2\pi f_c t \qquad \left(= \sqrt{\frac{2E_s}{T_s}}g(t)\cos(2\pi f_c t + \pi)\right) \tag{3.11}$$

over $0 \leq t \leq T_s$. The symbols in the signal constellation diagram for BPSK modulation are given by $s_1 = \sqrt{E_s}$ and $s_2 = -\sqrt{E_s}$ as shown in figure 3.2. From the figure, it is observed that the symbol energy is the square of the distance between the origin and the symbol. For BPSK, both the signals in the signal set have the same amount of energy as they are equidistant from the origin.

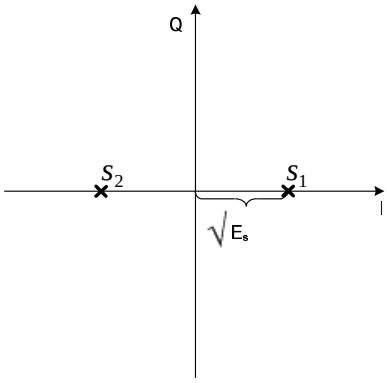

Figure 3.2: Signal constellation diagram for BPSK

Quaternary Phase Shift Keying

In Quaternary Phase Shift Keying (QPSK), two bits are transmitted simultaneously in a single modulation symbol, thereby doubling the bandwidth efficiency when compared to BPSK. The phase of the carrier takes one of four equally spaced values, such as $0, \frac{\pi}{2}, \pi$ and $\frac{3\pi}{2}$, where each value of phase corresponds to a unique pair of message bits. The signals in the signal set for such a QPSK system can be obtained by putting $M = 4$ into equations 3.3, 3.6 and 3.7, thus obtaining

$$s_1(t) = \sqrt{E_s}\phi_1(t) \tag{3.12}$$

$$= \sqrt{\frac{2E_s}{T_s}}g(t)\cos 2\pi f_c t \tag{3.13}$$

$$s_2(t) = \sqrt{E_s}\phi_2(t) \tag{3.14}$$

$$= -\sqrt{\frac{2E_s}{T_s}}g(t)\sin 2\pi f_c t \qquad \left(= \sqrt{\frac{2E_s}{T_s}}g(t)\cos(2\pi f_c t + \frac{\pi}{2})\right) \tag{3.15}$$

$$s_3(t) = -\sqrt{E_s}\phi_1(t) \tag{3.16}$$

$$= -\sqrt{\frac{2E_s}{T_s}}g(t)\cos 2\pi f_c t \qquad \left(= \sqrt{\frac{2E_s}{T_s}}g(t)\cos(2\pi f_c t + \pi)\right) \tag{3.17}$$

$$s_4(t) = -\sqrt{E_s}\phi_2(t) \tag{3.18}$$

$$= \sqrt{\frac{2E_s}{T_s}}g(t)\sin 2\pi f_c t \qquad \left(= \sqrt{\frac{2E_s}{T_s}}g(t)\cos(2\pi f_c t + \frac{3\pi}{2})\right) \tag{3.19}$$

The symbols in the signal constellation diagram for QPSK are given by $s_1 = \sqrt{E_s}$, $s_2 = j\sqrt{E_s}$, $s_3 = -\sqrt{E_s}$ and $s_4 = -j\sqrt{E_s}$ as shown in figure 3.3. Using a different set of carrier phases (separated by $\frac{\pi}{2}$) doesn't change the performance of the system but just rotates the signal constellation. One such QPSK constellation where the carrier phases used are $\frac{\pi}{4}$, $\frac{3\pi}{4}$, $\frac{5\pi}{4}$ and $\frac{7\pi}{4}$ is shown in figure 3.4. Another way of looking at QPSK is that it is nothing but

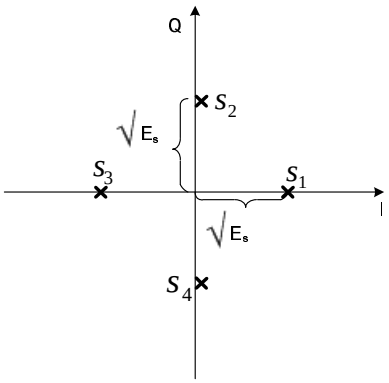

Figure 3.3: Signal constellation diagram for QPSK where the carrier phases are $0, \frac{\pi}{2}, \pi, \frac{3\pi}{2}$

two BPSK streams in parallel where the first stream is normal BPSK modulation and the second stream is like the first, but shifted by 90°. The first stream is the in-phase component and the second stream is the quadrature component. Since the two substreams are identical, the bit error performance of QPSK is the same as that of BPSK. Thus when compared to BPSK, QPSK provides twice the spectral efficiency with exactly the same energy efficiency.

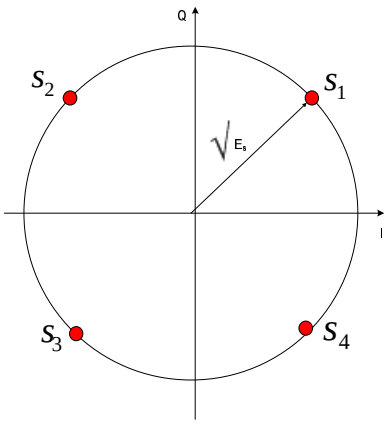

Figure 3.4: Signal constellation diagram for QPSK where the carrier phases are $\frac{\pi}{4}, \frac{3\pi}{4}, \frac{5\pi}{4}, \frac{7\pi}{4}$

3.1.2 Quadrature Amplitude Modulation

In BPSK and QPSK, the amplitude of the transmitted signal is constrained to remain constant, thereby yielding a circular constellation. In Quadrature Amplitude Modulation (QAM), the amplitude is also allowed to vary along with the phase thereby allowing it to be viewed as a combination of ASK and PSK, giving rise to the alternative name, *amplitude phase keying* (APK). M-QAM signals can be obtained by putting

$$x_{r,m} = \sqrt{E_s} a_m \cos\left[\frac{2\pi}{M}(m-1)\right] \tag{3.20}$$

$$x_{i,m} = \sqrt{E_s} b_m \sin\left[\frac{2\pi}{M}(m-1)\right] \tag{3.21}$$

into equation 3.3, where a_m and b_m are a pair of independent integers chosen according to the location of the particular signal point. For M-QAM, the (a_m, b_m) pair is an element of the $L \times L$ matrix

$$\begin{bmatrix} (-L+1, L-1) & (-L+3, L-1) & \dots & (L-1, L-1) \\ (-L+1, L-3) & (-L+3, L-3) & \dots & (L-1, L-3) \\ \vdots & \vdots & \vdots & \vdots \\ (-L+1, -L+1) & (-L+3, -L+1) & \dots & (L-1, L+1) \end{bmatrix} \tag{3.22}$$

where $L = \sqrt{M}$.

16-QAM

16-QAM is a form of QAM where four message bits are grouped together to form a single baseband message signal thus giving rise to 16 different signals in its signal set. The signals in a 16-QAM signal set are given by putting $M = 16$ into equations 3.3, 3.20, 3.21 and 3.22. For 16-QAM, the (a_m, b_m) pair is an element of the matrix

$$\begin{bmatrix} (-3,3) & (-1,3) & (1,3) & (3,3) \\ (-3,1) & (-1,1) & (1,1) & (3,1) \\ (-3,-1) & (-1,-1) & (1,-1) & (3,-1) \\ (-3,-3) & (-1,-3) & (1,-3) & (3,-3) \end{bmatrix} \tag{3.23}$$

and the signal constellation diagram is as shown in figure 3.5.

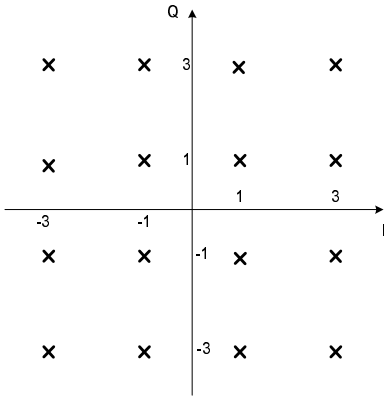

Figure 3.5: Signal constellation diagram for 16-QAM

64-QAM

64-QAM is similar to 16-QAM except that six message bits are grouped together in this case to form a single baseband message signal thus giving rise to 64 different signals in its signal set. The signals in a 64-QAM signal set are given by putting $M = 64$ into equations 3.3, 3.20, 3.21 and 3.22. Since more number of bits are carried by a single signal, the bandwidth efficiency increases but the energy efficiency decreases when compared to 16-QAM. The signal constellation diagram for 64-QAM is shown in figure 3.6.

The bandwidth efficiency of M-QAM is identical to M-ary PSK, but M-QAM has better error rate performance than M-ary PSK since the signals are spread farther apart in the

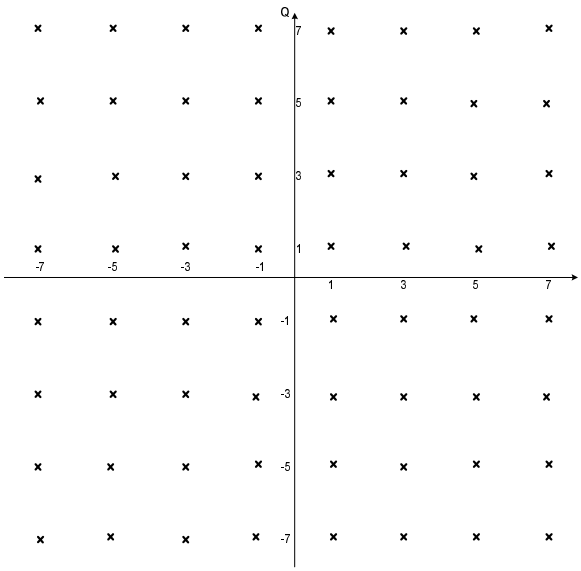

Figure 3.6: Signal constellation diagram for 64-QAM

M-QAM constellation. It can also be observed that all the symbols in M-QAM do not have the same energy as is the case in M-ary PSK.

3.1.3 Symbol Mapping

Symbol Mapping is the mapping of R information bits to the $M = 2^R$ possible symbols in a constellation. Mapping affects the bit error rate by determining how many bit errors occur each time there is a symbol error. *Gray mapping* is one such mapping technique which is used in this work. In Gray encoding, the adjacent symbols differ by one bit. Such a technique is used since the most likely errors caused by noise involve the erroneous selection of an adjacent symbol to the transmitted symbol. So, even if a symbol is erroneously decoded, only one bit is actually in error. This effectually minimizes the number of incorrectly received bits due to symbol errors. Signal constellations with Gray mapping for QPSK, 16-QAM and 64-QAM are shown in figure 3.7 (a), (b) and (c) respectively.

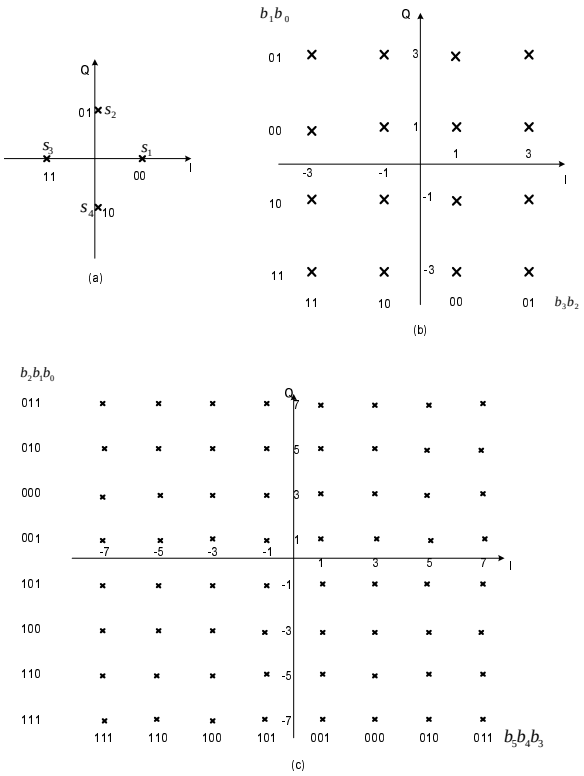

Figure 3.7: Gray mapping for QPSK, 16-QAM and 64-QAM

3.2 Forward Error Correction

Forward Error Correction is a type of *channel coding* technique where extra bits called *parity bits* are added to the actual bit stream to be transmitted, so that the receiver can correct errors caused by the channel using the parity bits.

Channel coding effectually introduces some redundancy, in a controlled manner, into the transmitted data stream and this redundancy can be used at the receiver to overcome the effects of noise and interference encountered in the transmission of the signal through the channel. Channel coding can be divided into two types: *waveform coding* and *structured sequences* [14]. Waveform coding transforms a waveform set that represents a message set into an improved waveform set which yields better detection performance over that of the original waveforms. The most popular of such waveform codes are the *orthogonal* and *bi-orthogonal* codes. Although waveform coding improves the error performance of the system, it also highly increases the required transmission bandwidth thereby degrading the band-

width efficiency of the system. Structured redundancy uses redundant bits either for error detection only or for both detection and correction of the errors occurred due to a noisy channel. When the errors could only be detected but not corrected, the communication system generally provides a retransmission technique called the *automatic repeat request* or *automatic retransmission query* (ARQ), which retransmits the erroneous messages. But such a retransmission technique requires a feedback link from the receiver to the transmitter. Forward error correction requires a one way link only since the parity bits in this case are designed for both the detection and correction of errors. Although the introduction of redundant bits reduces the bandwidth efficiency in this case too, it is not as high as in waveform coding. There are three basic types of forward error correction codes: *block codes, convolutional codes* and *turbo codes*.

Block codes enable a limited number of errors to be detected and corrected. In block codes, parity bits are added to blocks of message bits to make *codewords*. The encoder of a block code accepts blocks of k input data bits and produces blocks of n output code bits by adding $n-k$ redundant data bits. For a block of k input data bits, 2^k different codewords are possible. The block code is referred to as an *(n,k)* code and the rate of the code is defined as $r = \frac{k}{n}$ and is equal to the rate of information divided by the raw channel rate. The error detection and correction capability of a block code depends on its distance properties. The *minimum distance* of a block code is the smallest distance between any two codewords in the given codeword set. A code with minimum distance d_{min} can correct any combination of up to t errors, where $t = \lfloor \frac{d_{min}-1}{2} \rfloor$ is the *error correction capability* of the code. A code with minimum distance d_{min} can detect any combination of up to $(d_{min}-1)$ errors. d_{min} is desired to be as large as possible so that the codewords in a codeword set are as distinct as possible. Block codes are further classified into *Perfect Binary Codes*, *Imperfect Binary Codes* and *Non-binary codes*, and Reed-Solomon codes belong to the class of non-binary codes.

3.2.1 Reed-Solomon Codes

Reed-Solomon(R-S) codes are capable of correcting errors which appear in bursts and are commonly used in concatenated coding systems. Reed-Solomon code is specified as a

(n, k) code, where n is the number of symbols in the codeword that the R-S encoder outputs and k is the number of message symbols input to the encoder. Here $n = 2^m - 1$, where m is the number of bits per symbol. The error correction capability of a Reed-Solomon code is given by the formula $t = \lfloor \frac{n-k}{2} \rfloor$ and $2t$ is the number of parity symbols that the encoder adds to the stream of message symbols. The minimum distance of a Reed-Solomon code is given by $d_{min} = n - k + 1$. Reed-Solomon codes are said to have good distance properties as they can achieve larger values of d_{min} compared to many other codes. Reed-Solomon codes become more efficient as the code block size increases (keeping the code rate constant), and this property of the Reed-Solomon codes can be used efficiently when long block lengths are desired [14]. Also, as the redundancy of an R-S code increases, its bit error performance improves, but the complexity of its implementation also increases, especially in high speed devices.

Reed-Solomon codes are based on the arithmetic of finite fields, called Galois Fields. Galois Fields are denoted by $GF(p^m)$, where p is a prime number and m = number of bits per symbol. For Reed-Solomon codes, $p = 2$. So, if $m = 3$, the Galois Field used is $GF(2^3)$. The Galois Field elements range from 0 to $2^m - 1$. So, in the case when $m = 3$, the Galois Field set is $\{0, 1, 2, 3, 4, 5, 6, 7\}$. Every Galois Field $GF(2^m)$ can be generated using a primitive polynomial over $GF(2) = \{0, 1\}$. Every m has at least one primitive polynomial which can be used to generate the Galois Field. If α is a root of the primitive polynomial, all the Galois Field elements of $GF(2^m)$ except 0 and 1 can be represented as powers of α, i.e., $GF(2^m) = \{0, 1, \alpha, \alpha^2, ..\alpha^{n-1}\}$, where $n = 2^m - 1$. Different R-S encoder-decoder systems can have different primitive polynomials to generate the Galois Fields and these primitive polynomials are called *Field Generator Polynomials*. The *Code Generator Polynomial* $g(x)$ of a t-error correcting Reed-Solomon code is given by [15]

$$g(x) = (x - \alpha^j)(x - \alpha^{j+1})(x - \alpha^{j+2}).....(x - \alpha^{j+2t-1}) \tag{3.24}$$

Normally $j = 1$, but by varying j from 1 to n, we can have n different generator polynomials. The Reed-Solomon encoder uses the generator polynomial along with the input information symbols to produce a cyclic codeword polynomial of degree $n - 1$. The original information symbols are inserted at the higher order coefficients of the codeword polynomial and its lower

order coefficients are the parity symbols.

The WiMAX PHY uses a systematic R-S ($n = 255, k = 239$) code where the Galois Field elements are from $GF(2^8)$, i.e, $m = 8$ in this case. The primitive polynomial used in the WiMAX PHY is given by

$$p(x) = x^8 + x^4 + x^3 + x^2 + 1 \tag{3.25}$$

A Reed-Solomon encoder with the above given parameters is used in the present work.

3.2.2 Convolutional Codes

Convolutional codes differ from block codes in that instead of grouping the information sequences into distinct blocks and then encoding, here a continuous sequence of information bits is mapped into a continuous sequence of encoder output bits. For this reason, convolutional codes are widely implemented in real-time applications. A convolutional code can be thought of as a code with *memory* in the sense that the output of a convolutional encoder depends not only upon the present input, but also on the previous inputs. The input is passed through a *finite state shift register* which has already stored a finite number of past inputs and the output of the encoder is a linear combination of the present input and the contents of the shift register. A convolutional encoder is said to have a memory order of m if its shift register can hold m previous inputs.

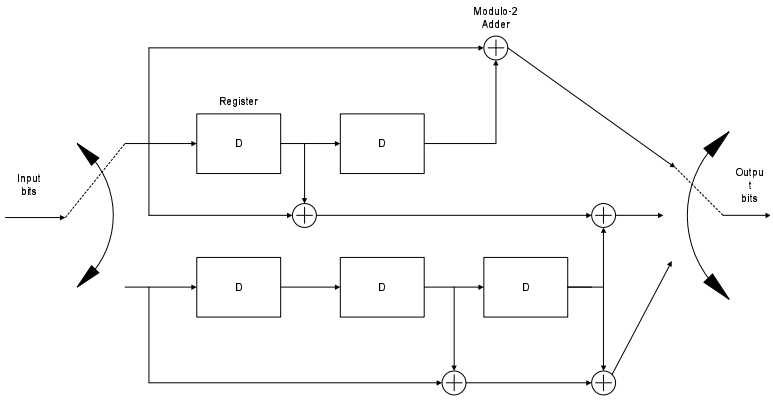

Figure 3.8: A convolutional encoder with memory order m=3

Figure 3.8 shows a convolutional encoder whose memory order $m = 3$. A convolutional encoder may have k input bit streams and n output bit streams. Each register holds k bits

(one taken from each of the input streams), and this set of k-bits is defined to be a *word*. The *constraint length* K of a convolutional encoder is the total number of k-bit words that each output depends on and is given by $K = m + 1$. A convolutional code with k input streams, n output streams and a constraint length of K is generally denoted as a (n, k, K) code. The convolutional encoder shown in figure 3.8 is a $(3, 2, 4)$ code. A convolutional encoder can also be represented by a set of $(k \times n)$ *generator polynomials*. For reasons of simplicity and also since the WiMAX PHY uses such an encoder, we will assume that we have an encoder with one input stream, i.e, k = 1. Such an encoder is shown in figure 3.9.

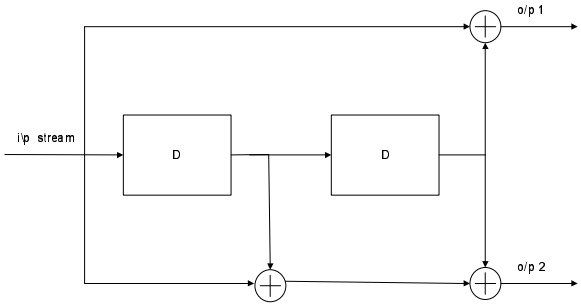

Figure 3.9: A convolutional encoder with a single input stream

The convolutional encoder in figure 3.9 has two outputs and for each output, one generator polynomial can be written. The generator polynomial's coefficients of an output are derived from which of the registers that particular output depends and whether it depends on the input. For the convolutional encoder shown in figure 3.9, the generator polynomials for output 1 and output 2 can be written as

$$g_0(D) = 1 + D^2 \tag{3.26}$$

and

$$g_1(D) = 1 + D + D^2 \tag{3.27}$$

respectively. The coefficients of the generator polynomials can be placed into a set of *generator vectors* where each generator vector consists of a 1 or 0 depending on the generator polynomial coefficients. For the convolutional encoder shown in figure 3.9, the generator vectors are $g_0 = [101]$ and $g_1 = [111]$, which can further be shown in a simplified octal representation as $(5, 7)$.

Decoding of convolutional codes is performed using the *Viterbi algorithm* [16] which uses the *maximum likelihood* decoding principle. For describing the Viterbi algorithm, a convolutional encoder is represented by a *trellis* diagram which explicitly shows the passage of time. In a trellis, the input data bits and output code bits are represented by a unique path through the trellis and all the possible states are shown for each instant of time, where a *state* is defined by the content of the memory (registers) at that particular instant of time. A part of the trellis diagram for a 4-state convolutional encoder is shown in figure 3.10.

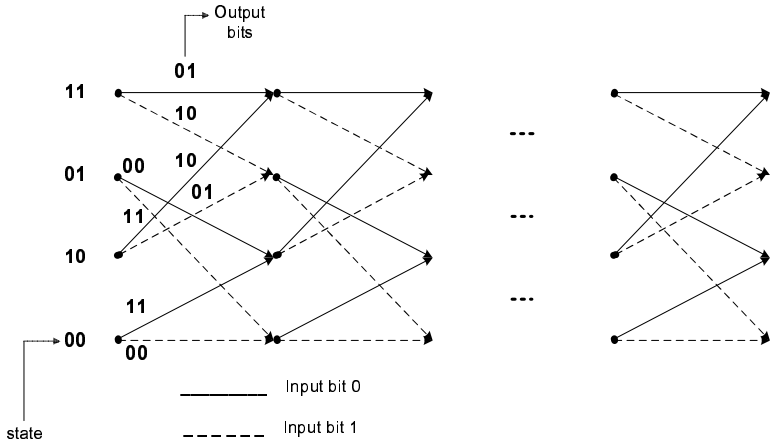

Figure 3.10: Trellis diagram for the $(5, 7)$ encoder shown in figure 3.9

The received sequence is compared against all the paths through the trellis and the path that is closest to the received sequence is chosen. As the received sequence is traversed through the trellis one stage at a time, a new path is chosen at the end of each stage whose code sequence differs least from the received sequence and all other paths leading into that stage are discarded. Once a valid full path that traverses all along the trellis is chosen, the decoded bits can be obtained by reading the input bits at every stage in the path. While *hard decision decoding* uses the hamming distance between the received sequence and the path sequence as the distance metric, *soft decision decoding* uses the squared Euclidean distance between them as the distance metric. Soft decision decoding is superior over hard decision decoding by about 2 to 3 dB. While the performance is limited by the minimum hamming distance (d_{min}) between distinct codewords in block codes, the performance is limited by the minimum distance between distinct paths through the trellis that start and end in the all

zeros state, called the *minimum free distance* (d_{free}), in convolutional codes [17].

The WiMAX PHY uses a rate 1/2, constraint length K = 7 convolutional code whose generator vectors are given by

$$g_0 = [1111001] \text{ for output 1} \tag{3.28}$$

$$g_1 = [1011011] \text{ for output 2} \tag{3.29}$$

as shown in figure 3.11 [18].

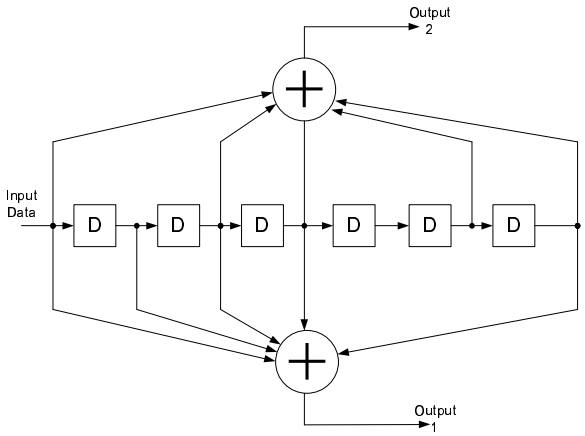

Figure 3.11: Convolutional encoder used in the WiMAX PHY

This convolutional encoder is used in the present work. Both Reed-Solomon codes and Convolutional codes provide a *coding gain* which is a measure of the amount of additional SNR that would be required to provide the same BER performance for an uncoded message signal in the same channel conditions.

Chapter 4

Space Time Block Codes and Orthogonal Frequency Division Multiplexing in WiMAX systems

4.1 Space Time Block Codes

In Space Time Block Codes (STBC), the data stream to be transmitted is encoded in *blocks* which are distributed among spaced antennas and across time. This distribution of transmitted symbols over multiple transmit antennas and different time slots can be represented in the form of a matrix as shown below.

$$timeslots \downarrow \begin{bmatrix} s_{1,1} & s_{1,2} & \dots & s_{1,n_t} \\ s_{2,1} & s_{2,2} & \dots & s_{2,n_t} \\ \vdots & \vdots & \vdots & \vdots \\ s_{T,1} & s_{T,2} & \dots & s_{T,n_t} \end{bmatrix} \quad (4.1)$$
$$\underset{antennas}{\rightarrow}$$

n_t is the number of transmit antennas and T is the number of time slots. Each row represents a time slot and each column represents one antenna's transmissions over time. While it is necessary to have multiple transmit antennas, it is not necessary to have multiple receive antennas, although to do so improves performance. Alamouti invented a simple transmit diversity technique with two transmit antennas [13] popularly known as the Alamouti STBC which provides full $n_t n_r$ diversity with little or no rate penalty. This technique uses the

maximum likelihood decoding at the receiver and is used in the present work to provide for antenna diversity.

Suppose we have two transmit and two receive antennas. Two different symbols s_1 and s_2 are transmitted from antenna 1 and antenna 2 respectively during the first time slot. During the second time slot, antenna 1 transmits $-s_2^*$ (negative conjugate of s_2) and antenna 2 transmits s_1^*. The transmitted symbol matrix can be represented as

$$\boldsymbol{S} = \begin{bmatrix} s_1 & s_2 \\ -s_2^* & s_1^* \end{bmatrix} \tag{4.2}$$

If $h_{t,r}$ is considered to be the complex channel response between transmit antenna t and receive antenna r, then the discrete-time received signals at antenna 1 during the two symbol intervals are

$$r_1^1 = h_{1,1}\frac{s_1}{\sqrt{2}} + h_{2,1}\frac{s_2}{\sqrt{2}} + n_1^1 \tag{4.3}$$

$$r_2^1 = -h_{1,1}\frac{s_2^*}{\sqrt{2}} + h_{2,1}\frac{s_1^*}{\sqrt{2}} + n_2^1 \tag{4.4}$$

and the corresponding signals at receive antenna 2 are

$$r_1^2 = h_{1,2}\frac{s_1}{\sqrt{2}} + h_{2,2}\frac{s_2}{\sqrt{2}} + n_1^2 \tag{4.5}$$

$$r_2^2 = -h_{1,2}\frac{s_2^*}{\sqrt{2}} + h_{2,2}\frac{s_1^*}{\sqrt{2}} + n_2^2 \tag{4.6}$$

where n_p^q is the noise sample at receive antenna q during the time slot p. The noise samples are independent and identically distributed complex Gaussian zero-mean random variables with power $\frac{N_0}{2}$. The vector received signal is formed by stacking the the scalar received signals as shown below.

$$\boldsymbol{r} = \begin{bmatrix} r_1^1 \\ (r_2^1)^* \\ r_1^2 \\ (r_2^2)^* \end{bmatrix} \tag{4.7}$$

It can be noticed that every other matched filter output is complex conjugated before creating the signal vector $\boldsymbol{r}$. Then the received signal vector can be shown as [4]

$$\boldsymbol{r} = \boldsymbol{H}\boldsymbol{s} + \boldsymbol{n} \tag{4.8}$$

where

$$\boldsymbol{H} = \begin{bmatrix} h_{1,1} & h_{2,1} \\ h_{2,1}^* & -h_{1,1}^* \\ h_{1,2} & h_{2,2} \\ h_{2,2}^* & -h_{1,2}^* \end{bmatrix} \tag{4.9}$$

$$\boldsymbol{s} = \frac{1}{\sqrt{2}} \begin{bmatrix} s_1 \\ s_2 \end{bmatrix} \tag{4.10}$$

and

$$\boldsymbol{n} = \begin{bmatrix} n_1^1 \\ (n_2^1)^* \\ n_1^2 \\ (n_2^2)^* \end{bmatrix} \tag{4.11}$$

The columns of $\boldsymbol{H}$ are seen to be orthogonal and this is the key aspect of Alamouti STBC's effectiveness. At the receiver, a decision statistic vector $\boldsymbol{d}$ is formed by matched filtering the received signal vector with respect to the channel.

$$\begin{aligned} \boldsymbol{d} &= \boldsymbol{H}^H \boldsymbol{r} && (4.12) \\ &= \boldsymbol{H}^H (\boldsymbol{H}\boldsymbol{s} + \boldsymbol{n}) && (4.13) \\ &= \begin{bmatrix} E_h & 0 \\ 0 & E_h \end{bmatrix} \boldsymbol{s} + \boldsymbol{H}^H \boldsymbol{n} && (4.14) \\ &= E_h \boldsymbol{s} + \boldsymbol{v} && (4.15) \end{aligned}$$

where

$$E_h = |h_{1,1}|^2 + |h_{1,2}|^2 + |h_{2,1}|^2 + |h_{2,2}|^2 \tag{4.16}$$

and

$$\boldsymbol{v} \sim \mathcal{N}_c \left(\underline{0}, \frac{E_h N_0}{2} \boldsymbol{I} \right) \tag{4.17}$$

Since $\boldsymbol{H}^H\boldsymbol{H}$ is diagonal, there is no intersymbol interference, i.e., the decision statistics of each of the symbols do not depend upon the other symbol as shown in equations 4.18 and 4.19.

$$d_1 = [\boldsymbol{d}]_1 = \frac{E_h}{\sqrt{2}}s_1 + v_1 \tag{4.18}$$

$$d_2 = [\boldsymbol{d}]_2 = \frac{E_h}{\sqrt{2}}s_2 + v_2 \tag{4.19}$$

where v_1 and v_2 are Gaussian with mean 0 and variance $\sigma_d^2 = \frac{E_h N_0}{2}$, $\frac{N_0}{2}$ being the variance of the noise samples. The final maximum likelihood estimates are given by

$$\hat{s_1} = \arg \min_{s \in \boldsymbol{S}} |d_1 - s|^2 \tag{4.20}$$

$$\hat{s_2} = \arg \min_{s \in \boldsymbol{S}} |d_2 - s|^2 \tag{4.21}$$

Since this scheme transmits two symbols in two time slots, the rate of code is 1, i.e., there is no sacrifice in bandwidth to achieve full transmit antenna diversity. However, there is a 3 dB SNR loss since the transmit power is distributed across the two antennas. This scheme is useful when high throughput is required at low SNR. Alamouti's scheme works only for the two transmit antenna case when complex symbols are used. There are no full rate space-time block code matrices for more than two transmit antennas when complex symbols are used. Tarokh *et al* provided examples of lower rate code matrices that provide full diversity when complex symbols are used [19]. There exists full rate space time block codes only for 2, 4 and 8 transmit antennas when the symbols are real.

In the STBC scheme, the receiver assumes that each received signal is composed of a linear superposition of current symbols corrupted by noise. But in channel conditions where there is high delay spread, such assumption is not entirely valid since there exists a channel-induced ISI component and the performance of STBC might be sensitive to such environments. Since there is no memory between consecutive blocks and since the block length is very short, a very little coding gain can be expected. Since the scheme has a very simple decoder structure, it can be concatenated to a powerful outer error correction code [20]. In the present work, the STBC scheme is concatenated with an outer convolutional

code which does soft decision decoding using the Viterbi algorithm. The Viterbi algorithm used requires soft inputs to be input into it which necessitates the need for calculating the bitwise loglikelihood ratios (LLR) of the received symbols. The calculation of bitwise LLRs of the received symbols in an STBC system is explained in the following section.

4.1.1 Bitwise LLR calculations for an STBC system

The modulations used in the present work are BPSK and QPSK. So the bitwise LLRs of the received symbols when BPSK and QPSK symbols are transmitted is calculated.

BPSK

With BPSK modulation, each of the two transmitted symbols in the block can be either 1 or -1, where it is assumed that either symbol has unit energy. Let s be one of the symbols transmitted and let d be its decision statistic. The log-likelihood ratio can be calculated from d using the equation

$$\lambda(d) = \ln\left(\frac{p\left(d|s=1,\boldsymbol{H}\right)}{p\left(d|s=-1,\boldsymbol{H}\right)}\right) \tag{4.22}$$

Now d is a Gaussian random variable with mean $\frac{1}{\sqrt{2}}E_h s$ and variance σ_d^2. Therefore

$$\begin{aligned}
\lambda(d) &= \ln\left[\frac{\frac{1}{\sigma_d\sqrt{2\pi}}\exp\left(-\frac{\left(d-\frac{E_h}{\sqrt{2}}\right)^2}{2\sigma_d^2}\right)}{\frac{1}{\sigma_d\sqrt{2\pi}}\exp\left(-\frac{\left(d+\frac{E_h}{\sqrt{2}}\right)^2}{2\sigma_d^2}\right)}\right] && (4.23)\\
&= \ln\left[\exp\left(\frac{\left(d+\frac{E_h}{\sqrt{2}}\right)^2-\left(d-\frac{E_h}{\sqrt{2}}\right)^2}{2\sigma_d^2}\right)\right] && (4.24)\\
&= \frac{\sqrt{2}dE_h}{\sigma_d^2} && (4.25)\\
&= \frac{\sqrt{2}dE_h}{E_h\frac{N_0}{2}} && (4.26)\\
&= \frac{2\sqrt{2}d}{N_0} && (4.27)
\end{aligned}$$

If $\lambda(d) > 0$, then $s = 1$, else $s = -1$. Thus the bit transmitted can be found according to which symbol is transmitted for a bit 0 or bit 1.

QPSK

With QPSK modulation, each of the two transmitted symbols in the block can be one from $1, -1, j, -j$, where it is assumed that all the symbols have unit energy. Using Gray mapping, pairs of bits are mapped to the QPSK symbols in the following manner:

$$00 \rightarrow 1 \qquad 01 \rightarrow j \qquad 11 \rightarrow -1 \qquad 10 \rightarrow -j$$

Next, the symbols are grouped into sets according to whether their first and second bits represent a 0 or a 1 in the following manner:

$S_1^0 = \{1, j\}$ is the set of symbols whose first bit is a 0

$S_1^1 = \{-1, -j\}$ is the set of symbols whose first bit is a 1

$S_2^0 = \{1, -j\}$ is the set of symbols whose second bit is a 0

$S_2^1 = \{-1, j\}$ is the set of symbols whose second bit is a 1

Let s be one of the symbols transmitted and d be its decision statistic. Then log-likelihood ratio of the k^{th} bit (λ_k) is given by [21]

$$\lambda_k = \ln \left[\frac{\Sigma_{s \in S_k^1} p(s|d)}{\Sigma_{s \in S_k^0} p(s|d)} \right] \tag{4.28}$$

where $p(s|d)$ is the conditional pdf of s given d. Applying the Bayes' rule, equation 4.28 can be written as

$$\lambda_k = \ln \left[\frac{\Sigma_{s \in S_k^1} p(d|s)}{\Sigma_{s \in S_k^0} p(d|s)} \right] \tag{4.29}$$

when symbols are equally likely. Therefore LLR for the first bit is

$$\lambda_1(d) = \ln \left[\frac{p(d|s=-1) + p(d|s=-j)}{p(d|s=1) + p(d|s=j)} \right] \tag{4.30}$$

Similarly, LLR for the second bit is

$$\lambda_2(d) = \ln \left[\frac{p(d|s=-1) + p(d|s=j)}{p(d|s=1) + p(d|s=-j)} \right] \tag{4.31}$$

Now we find the conditional pdf of d for different values of s. Suppose s = 1, then

$$d = \frac{E_h}{\sqrt{2}} + v \tag{4.32}$$

$$= \frac{E_h}{\sqrt{2}} + (v_r + j v_i) \tag{4.33}$$

where $v = v_r + jv_i$ is the complex Gaussian noise. d is a complex number that can be broken into real and imaginary parts d_r and d_i where

$$d_r = \frac{E_h}{\sqrt{2}} + v_r \tag{4.34}$$

and

$$d_i = v_i \tag{4.35}$$

d_r is a Gaussian random variable with mean $\frac{E_h}{\sqrt{2}}$ and variance σ_d^2. Therefore conditional pdf of d_r is given by

$$p(d_r|s=1) = \frac{1}{\sigma_d\sqrt{2\pi}} \exp\left[\frac{-\left(d_r - \frac{E_h}{\sqrt{2}}\right)^2}{2\sigma_d^2}\right] \tag{4.36}$$

Similarly d_i is a Gaussian random variable with mean 0 and variance σ_d^2. So the conditional pdf of d_i is given by

$$p(d_i|s=1) = \frac{1}{\sigma_d\sqrt{2\pi}} \exp\left[\frac{-d_i^2}{2\sigma_d^2}\right] \tag{4.37}$$

Since the real and imaginary parts of d are independent, the conditional pdf of d as a whole can be written as

$$\begin{aligned}
p(d|s=1) &= p(d_r|s=1).p(d_i|s=1) && (4.38)\\
&= \left(\frac{1}{2\pi\sigma_d^2}\right) \exp\left[\frac{-\left(\left(d_r - \frac{E_h}{\sqrt{2}}\right)^2 + d_i^2\right)}{2\sigma_d^2}\right] && (4.39)\\
&= \left(\frac{1}{2\pi\sigma_d^2}\right) \exp\left[\frac{-\left|\left(d_r - \frac{E_h}{\sqrt{2}}\right) + jd_i\right|^2}{2\sigma_d^2}\right] && (4.40)\\
&= \left(\frac{1}{2\pi\sigma_d^2}\right) \exp\left[\frac{-\left|(d_r + jd_i) - \frac{E_h}{\sqrt{2}}\right|^2}{2\sigma_d^2}\right] && (4.41)\\
&= \left(\frac{1}{\pi E_h N_0}\right) \exp\left[\frac{-\left|d - \frac{E_h}{\sqrt{2}}\right|^2}{E_h N_0}\right] && (4.42)
\end{aligned}$$

By similar calculations, it can be shown that

$$p(d|s=-1) = \left(\frac{1}{\pi E_h N_0}\right) \exp\left[\frac{-\left|d+\frac{E_h}{\sqrt{2}}\right|^2}{E_h N_0}\right] \tag{4.43}$$

$$p(d|s=j) = \left(\frac{1}{\pi E_h N_0}\right) \exp\left[\frac{-\left|d-\frac{jE_h}{\sqrt{2}}\right|^2}{E_h N_0}\right] \tag{4.44}$$

$$p(d|s=-j) = \left(\frac{1}{\pi E_h N_0}\right) \exp\left[\frac{-\left|d+\frac{jE_h}{\sqrt{2}}\right|^2}{E_h N_0}\right] \tag{4.45}$$

By plugging in the above calculated conditional probability density functions into equations 4.30 and 4.31, we get the bitwise LLRs as

$$\lambda_1(d) = \ln\left[\frac{\exp\left(\frac{-\left|d+\frac{E_h}{\sqrt{2}}\right|^2}{E_h N_0}\right) + \exp\left(\frac{-\left|d+\frac{jE_h}{\sqrt{2}}\right|^2}{E_h N_0}\right)}{\exp\left(\frac{-\left|d-\frac{E_h}{\sqrt{2}}\right|^2}{E_h N_0}\right) + \exp\left(\frac{-\left|d-\frac{jE_h}{\sqrt{2}}\right|^2}{E_h N_0}\right)}\right] \tag{4.46}$$

and

$$\lambda_2(d) = \ln\left[\frac{\exp\left(\frac{-\left|d+\frac{E_h}{\sqrt{2}}\right|^2}{E_h N_0}\right) + \exp\left(\frac{-\left|d-\frac{jE_h}{\sqrt{2}}\right|^2}{E_h N_0}\right)}{\exp\left(\frac{-\left|d-\frac{E_h}{\sqrt{2}}\right|^2}{E_h N_0}\right) + \exp\left(\frac{-\left|d+\frac{jE_h}{\sqrt{2}}\right|^2}{E_h N_0}\right)}\right] \tag{4.47}$$

4.2 Orthogonal Frequency Division Multiplexing

Orthogonal Frequency Division Multiplexing (OFDM) is a bandwidth efficient, multi-carrier transmission technique that is tolerant to channel disturbances such as multipath fading. In OFDM, a high rate serial data stream is split up into a set of low-rate sub-streams, each of which is modulated on a separate subcarrier. By lowering the rate of the stream, the symbol duration is increased so that it is longer compared to the delay spread of the time-dispersive channel. Another way of looking at it is that by lowering the rate of the

stream, the bandwidth of the subcarrier is squeezed so that it is small compared with the coherence bandwidth of the channel, thereby making the individual subcarriers experience flat fading, which requires simple equalization techniques. Thus OFDM effectually converts a frequency-selective fading channel into a set of parallel flat fading channels. Lowering the rate of the substreams can be compensated for by selecting a set of *orthogonal* subcarriers whose spectra overlap, but at the same time do not interfere with each other, thereby avoiding inter-channel interference [22]. The orthogonality allows simultaneous transmission on a lot of subcarriers in a tight frequency space without interfering with each other.

Let N be the number of carriers available in the OFDM system and one PSK or QAM symbol is transmitted per carrier. One OFDM symbol consists of N PSK or QAM symbols whose symbol duration is T. The continuous-time baseband signal transmitted over the channel over symbol interval $[0, T]$ is given by [23]

$$s(t) = \sum_{k=0}^{N-1} s_k e^{j2\pi \frac{k}{T} t} \tag{4.48}$$

Expanding $s(t)$,

$$s(t) = s_0 + s_1 e^{j2\pi \frac{t}{T}} + s_2 e^{j2\pi \frac{2t}{T}} + \ldots + s_{N-1} e^{j2\pi \frac{(N-1)t}{T}} \qquad 0 \leq t \leq T \tag{4.49}$$

It can be seen that symbol s_i modulates a low frequency complex sinusoid with frequency $\frac{i}{T}$ and the subcarriers are separated by $\frac{1}{T}$. The subcarriers range from 0 Hz to $\frac{N-1}{T}$ and each subcarrier has an integer number of cycles in T, given by $0, 1, \ldots, N-1$. In frequency domain , this translates to the subcarriers having a sinc shape ($\frac{sinx}{x}$) with nulls spaced by the symbol rate so that the carriers fit in the nulls of other carriers thereby avoiding inter-carrier interference.

Weinstein and Ebert in [24] proposed the use of Discrete Fourier Transforms (DFT) for generating the different individual orthogonal carriers and modulating the symbols onto them. For a sufficiently large number of subcarriers, which translate directly to DFT points, the computation of the DFT is made even more efficient with the use of the fast Fourier Transform (FFT). The FFT basically calculates the spectral content of the signal. It moves a signal from the time domain where it is expressed as a series of time events to the frequency domain where it is expressed as the amplitude and phase of a particular frequency. The

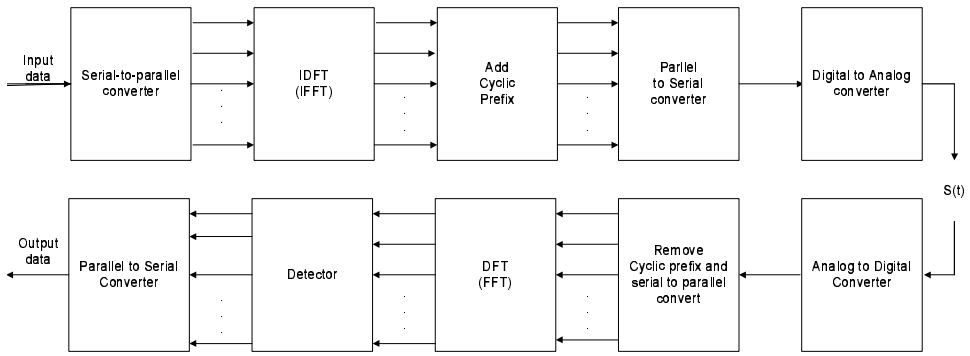

Figure 4.1: OFDM transmission system

inverse FFT used for OFDM demodulation at the receiver side performs the reciprocal operation. Usually, N is taken as a power of 2 to enable the application of the highly efficient FFT algorithms.

Cyclic Prefix is inserted between the OFDM symbols as guard interval to avoid inter-symbol interference. The cyclic prefix is a copy of the last part of the OFDM symbol which is transmitted before the actual OFDM symbol itself. This guards the symbol by being interfered from delayed copies of the previous symbols. The length of the cyclic prefix should exceed the maximum excess delay of the multipath propagation channel. Usually the cyclic prefix is selected to have a length of one tenth to a quarter of the symbol period. Suppose the length of the cyclic prefix is $\nu + 1$ signal samples, where $\nu \ll N$. After the IFFT operation, the last ν samples of the IFFT output are copied back as prefix to the IFFT output itself. So if $\{s_0, s_1, \ldots, s_{N-1}\}$ is the IFFT output sequence, after adding the cyclic prefix, the sequence would be $\{s_{N-\nu}, s_{N-\nu+1}, s_{N-\nu+2}, \ldots, s_{N-1}, s_0, s_1, \ldots, s_{N-1}\}$. At the receiver, the first ν samples are discarded so that the received sequence $r[n]$ is defined over $n = 0, 1, 2, \ldots, N-1$ and this sequence is passed to the N- point DFT to recover the transmitted sequence. Due to the cyclic prefix, the transmitted signal becomes periodic, and the effect of the time dispersive multipath channel becomes equivalent to a cyclic convolution, discarding the GI at the receiver [22]. Due to the properties of cyclic convolution, the effect of the multipath channel is limited to a pointwise multiplication of the transmitted data constellations by the channel transfer function, i.e., the subcarriers remain orthogonal.

Chapter 5

Results and Conclusions

This chapter presents the performance of the wireless communication system implemented in terms of its bit error rate (BER) with respect to the signal to noise ratio (SNR). SNR is given by $\frac{E_b}{N_0}$, where E_b is the energy per bit and $\frac{N_0}{2}$ is the two-sided noise spectral density.

5.1 Results

We first start by presenting the performance of the system in AWGN and flat fading channels when none of the diversity techniques are used. Later on, we begin to add each diversity technique and show the improvement in performance.

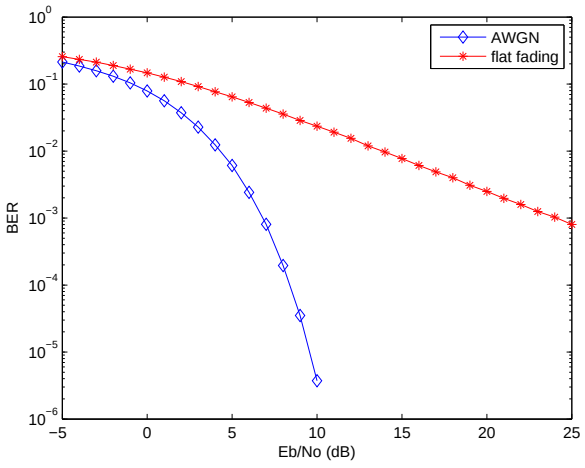

Figure 5.1: BER performance of the system when QPSK modulation is used and no error reduction techniques are implemented

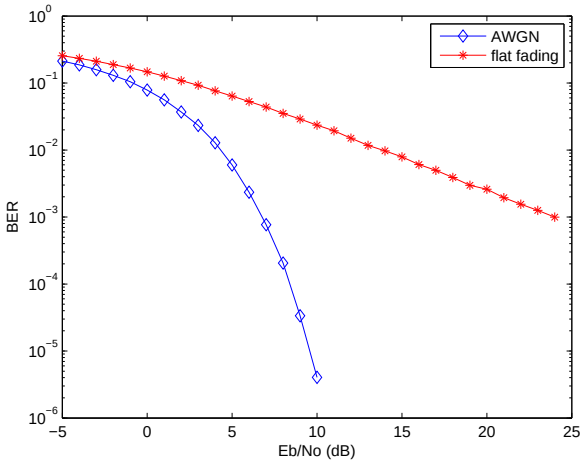

Figure 5.2: BER performance of the system when BPSK modulation is used and no error reduction techniques are implemented

Figures 5.1 and 5.2 show the BER performance of the system when QPSK and BPSK modulations are used respectively with no channel coding and diversity techniques employed. Here, the fading coefficient is varied for every symbol transmitted, i.e., different transmitted symbols see different fading conditions. Next we show how the performance of the system changes in flat fading conditions with the usage of different techniques.

5.1.1 Space Time Block Codes

Alamouti Space Time Block Codes using 2 antennas at the transmitter and 1 and/or 2 antennas at the receiver is implemented. For Alamouti STBC, the channel is assumed to be quasi-static, i.e., the fading coefficients between the transmit and receive antennas are held constant during the two time slots the symbols are transmitted. Figures 5.3 and 5.4 show the performance of the system varies with the usage of Alamouti STBC in flat fading conditions.

It can be observed that a diversity gain is achieved and increasing the number of receive antennas increase the performance of the system.

5.1.2 Convolutional codes

The variation in the performance of the system with the usage of a channel coding technique such as the convolutional coding is presented next. As discussed in chapter 3

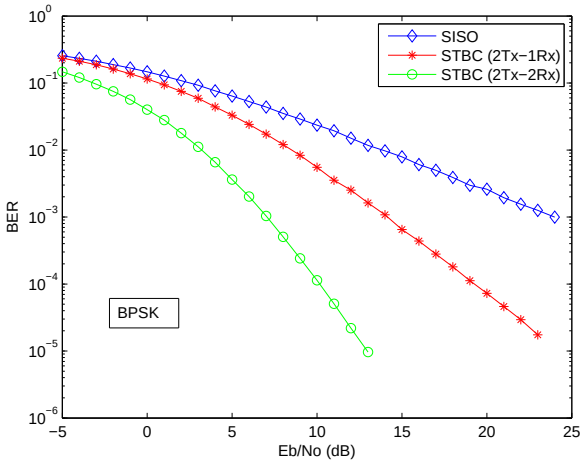

Figure 5.3: BER performance of the BPSK modulated system when Alamouti STBC is implemented

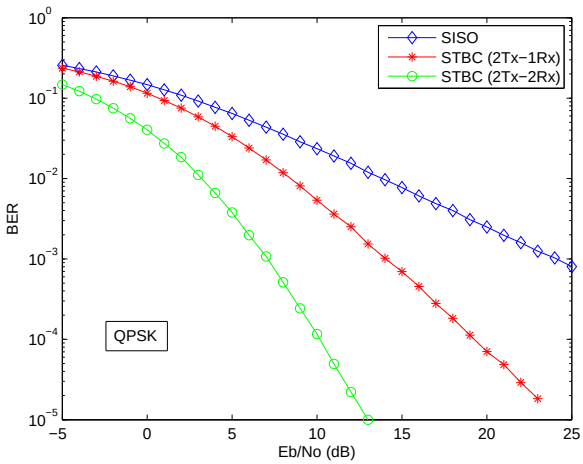

Figure 5.4: BER performance of the QPSK modulated system when Alamouti STBC is implemented

(section 3.2.2), a rate 1/2, constraint length $K = 7$ convolutional code whose generator vectors are given by

$$g_0 = [1111001] \text{ for output 1} \tag{5.1}$$

$$g_1 = [1011011] \text{ for output 2} \tag{5.2}$$

is used.

Figures 5.5 and 5.6 show the variation in the system's performance when channel coding is implemented via convolutional coding and it can be clearly observed that a coding gain is

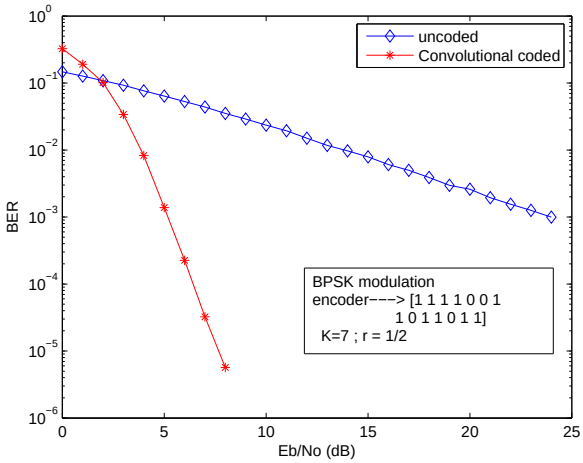

Figure 5.5: BER performance of the BPSK modulated system when Convolution coding is added

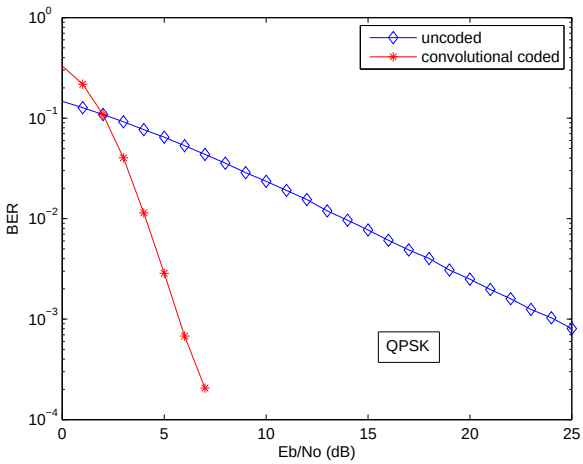

Figure 5.6: BER performance of the QPSK modulated system when Convolutional coding is added

achieved.

5.1.3 Reed-Solomon codes

As described previously, Reed-Solomon code is used in concatenation with inner Convolutional code to provide further coding gain. A systematic R-S $(n = 255, k = 239)$ code where the Galois Field elements are from $GF(2^8)$, i.e, $m = 8$ is used as the outer Reed-Solomon code in this work.

Figures 5.7 and 5.8 show the performance of the system when concatenated Reed-

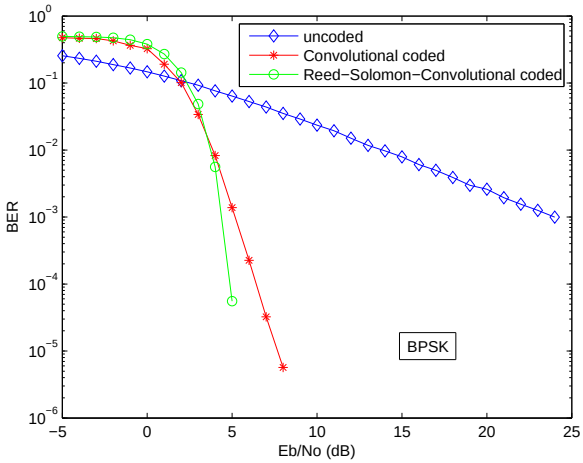

Figure 5.7: BER performance of the BPSK modulated system when concatenated Reed-Solomon-Convolution coding is added

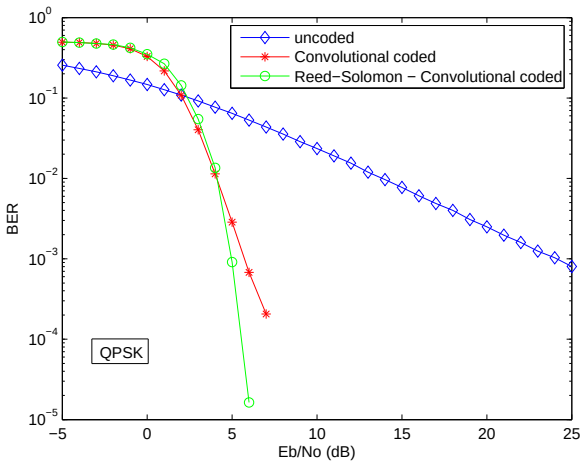

Figure 5.8: BER performance of the QPSK modulated system when concatenated Reed-Solomon Convolutional coding is added

Solomon-Convolutional coding is implemented in the system. It can be observed that Reed-Solomon codes provide additional coding gain to what can be achieved by using only convolutional coding. Reed-Solomon codes can themselves provide enormous gain even when not concatenated with a convolutional code, but concatenated with a Alamouti STBC system as can be observed from figures 5.9 and 5.10

Thus combining the features of Reed-Solomon codes, Convolutional codes and Alamouti STBC, a robust system that provides high coding gain and diversity gain is developed.

Figures 5.11 and 5.12 show the performance of the system for QPSK and BPSK modu-

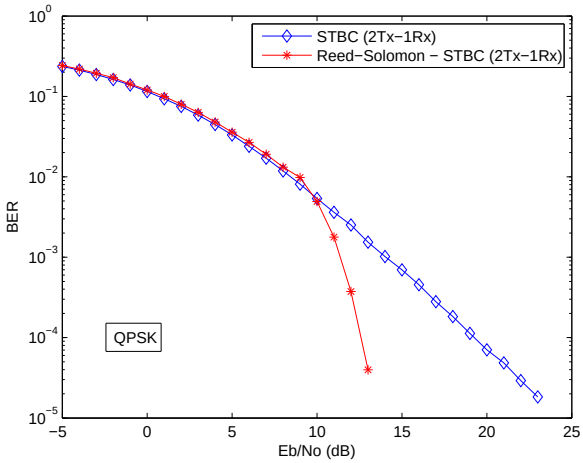

Figure 5.9: BER performance of the QPSK modulated system when Reed-Solomon coding is used along with STBC 2Tx-1Rx

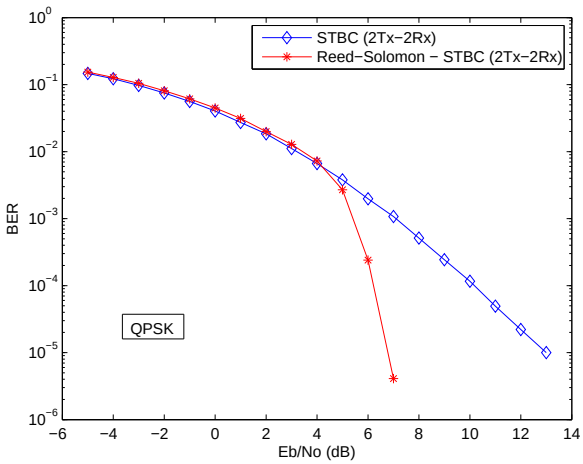

Figure 5.10: BER performance of the QPSK modulated system when Reed-Solomon coding is used along with STBC 2Tx-2Rx

lations respectively when time diversity and spatial diversity techniques are employed. The above figures show the performance of the system in only flat fading channels. Frequency selective channels severely degrade the performance of the present system and they are countered by introducing OFDM into the present system.

5.1.4 OFDM

As mentioned earlier, OFDM is a frequency diversity technique that converts a frequency-selective fading channel into a set of parallel flat fading channels onto which other diversity

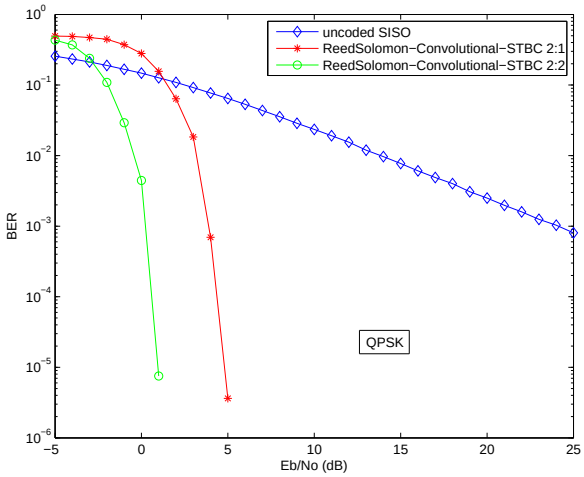

Figure 5.11: BER performance of the QPSK modulated system when concatenated Reed-Solomon-Convolutional coding is used along with Alamouti STBC

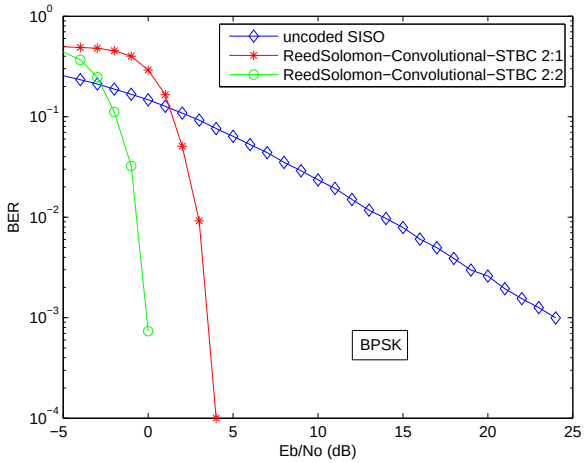

Figure 5.12: BER performance of the BPSK modulated system when concatenated Reed-Solomon-Convolutional coding is used along with Alamouti STBC

techniques can be applied. OFDM systems utilizing error-correction coding are often referred as coded OFDM (COFDM) systems. Combining the OFDM transmission technique with the Alamouti STBC technique yields a *space-frequency coded* orthogonal frequency division multiplexing technique [25] whose working model is described below with the help of figure 5.13.

In figure 5.13, C_1 and C_2 are two different sets of symbols each containing a number of symbols equal to the number of carriers used. Since a 256-carrier OFDM system is used here, C_1 and C_2 consist of 256 symbols each which are transmitted on the 256 carriers.

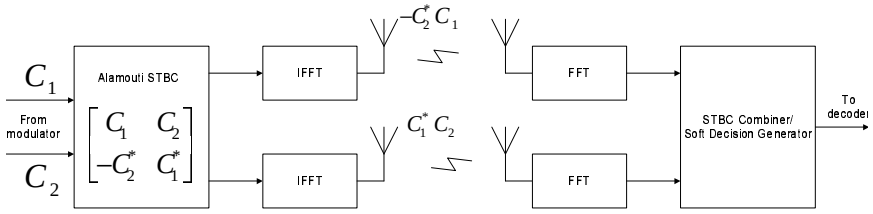

Figure 5.13: Space-frequency coded OFDM system

At a given symbol period, the OFDM block transmitted from the first antenna is $C_1 = c_1[1]\ c_1[2]\ c_1[3] \ldots c_1[K]$ and the OFDM block transmitted from the second antenna is $C_2 = c_2[1]\ c_2[2]\ c_2[3] \ldots c_2[K]$, where $c_i[p]$ is the symbol from the i th OFDM block transmitted on the p th carrier and K is the number of carriers. During the next symbol period, the block $-C_2^*$ is transmitted from the first antenna and the block C_1^* is transmitted from the second antenna. Fading is assumed to be quasi-static over the two symbol periods, i.e., the fading coefficients on different frequencies between a transmit-receive antenna pair are held constant during this period. The soft estimates for transmitted signals $c_1[k]$ and $c_2[k]$ at the j th receive antenna can be calculated from [13] and are given by [25]

$$\begin{bmatrix} \tilde{c}_1^j[k] \\ \tilde{c}_2^j[k] \end{bmatrix} = \sqrt{E_s} \begin{bmatrix} |H_{1j}[k]|^2 + |H_{2j}[k]|^2 & 0 \\ 0 & |H_{1j}[k]|^2 + |H_{2j}[k]|^2 \end{bmatrix} \times \begin{bmatrix} c_1[k] \\ c_2[k] \end{bmatrix} + \begin{bmatrix} n_{1j}[k] \\ n_{2j}[k] \end{bmatrix} \quad (5.3)$$

where $H_{ij}[k]$ denotes the normalized channel frequency response for the k th tone, corresponding to the channel between the i th transmit antenna and the j th receive antenna and E_s is the transmitted symbol energy. The performance of this space-frequency coded system, when combined with the Reed-Solomon -Convolutional code FEC, is shown in figures 5.14 and 5.15 for BPSK and QPSK modulations respectively.

5.2 Conclusion

From the results given in the previous section, it can be concluded that the Space-Frequency Coded system coupled with Reed-Solomon codes and Convolutional codes used in the WiMAX PHY efficiently exploits the time diversity, spatial diversity and frequency diversity offered by the fading channel and provides high performance at low SNRs. Thus the

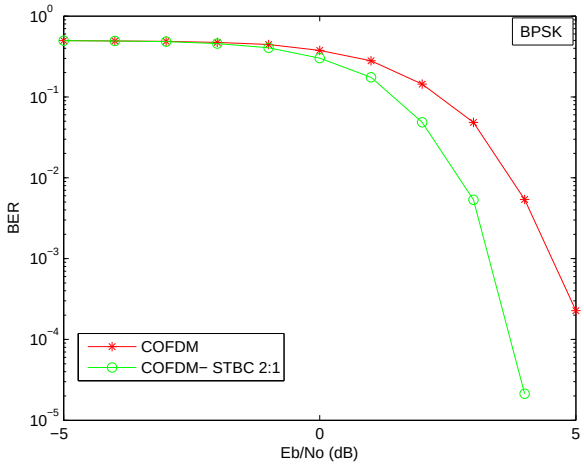

Figure 5.14: BER performance of the BPSK modulated system when concatenated Reed-Solomon-Convolutional coding is used along with the space-frequency coded system

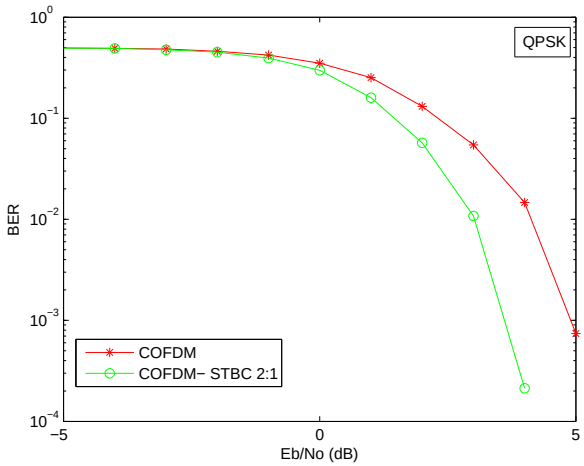

Figure 5.15: BER performance of the QPSK modulated system when concatenated Reed-Solomon-Convolutional coding is used along with the space-frequency coded system

present work overviews the key aspects of the IEEE 802.16 Physical layer and demonstrates their functionality and value to the WiMAX system.

References

[1] James E.Gaskin, *Broadband Bible*, Wiley Publishing Inc., Indianapolis, Indiana, USA., 2004.

[2] T.S. Rappaport, *Wireless Communications*, Prentice-Hall, Upper Saddle River, NJ, USA., 1996.

[3] M.C. Valenti, "Wireless networking," Course notes, WVU, Fall 2004.

[4] D. Reynolds, "Wireless communication systems," Course notes, WVU, Fall 2005.

[5] B. Sklar, "Rayleigh fading Channels in mobile digital communication systems. Part-I : characterization," *IEEE Commun. Magazine*, vol. 35, no. 9, pp. 136–146, Sept. 1997.

[6] P.A.Bello, "Characterization of Randomly Time-Variant Linear Channels," *IEEE Trans. Commun Sys.*, vol. CS-11, no. 49, pp. 360–393, Dec. 1963.

[7] Arunabha Ghosh, David R. Wolter, Jeffrey G. Andrews and Runhua Chen, "Broadband Wireless Access with WiMax/802.16: Current Performance Benchmarks and Future Potential," *IEEE Commun. Magazine*, vol. 43, no. 2, pp. 129–136, Feb. 2005.

[8] J.G. Proakis, *Digital Communications*, 3rd ed., New York, NY: McGraw-Hill, 1995.

[9] L. Zheng, D. Tse, "Diversity and multiplexing: A fundamental tradeoff in multiple antenna channels," vol. 49, pp. 1073–1096, May 2003.

[10] İ. Telatar, "Capacity of multi-antenna gaussian channels," vol. 10, no. 6, pp. 585–595, Nov. 1999.

[11] G. Foschini, "Layered space-time architecture for wireless communication in a fading environment when using multi-element antennas.," *Bell Labs. Tech. Journal*, vol. 1, no. 2, pp. 41–59, Autumn 1996.

[12] R. Heath, Jr. and A. Paulraj,, "Switching between multiplexing and diversity based on constellation distance,," in *Proc. Allerton Conf. Communication,Control and Computing,.*

[13] S. Alamouti, "A simple transmit diversity technique for wireless communications," vol. 16, no. 8, pp. 1451–1458, Oct. 1998.

[14] Bernard Sklar, *Digital Communications : Fundamentals and Applications* , 2nd ed., Upper Saddle River, NJ: Prentice Hall, 2002.

[15] Syed Shahzad Shah, Saqib Yaqub, and Faisal Suleman,, "Self-correcting codes conquer noise Part 2: Reed-Solomon codecs," pp. 107–120, March. 2001.

[16] A.J.Viterbi, "Error bounds for convolutional codes and an asymptotically optimum decoding algorithm," .

[17] M.C. Valenti, "Coding theory," Course notes, WVU, Spring 2006.

[18] IEEE Computer Society and IEEE Microwave Theory and Techniques, "IEEE Standard for Local and metropolitan area networks - Part 16 : Air Interface for Fixed Broadband Wireless Access Systems," .

[19] V. Tarokh, H. Jafarkhami, and A. R. Calderbank, "Space-time block codes from orthogonal designs,," *IEEE Trans. Inform. Theory*, vol. 45, no. 5, pp. 1456–1467, July 1999.

[20] Brian D.Woerner, "Multiple antenna systems," Course notes, WVU, Spring 2005.

[21] Tarik Ghanim and Matthew C.Valenti, "The throughput of Hybrid ARQ in block fading under modulation constraints," in *Information Sciences and Systems,.*

[22] Ramjee Prasad, *OFDM for Wireless Communication Systems* , Artech House Publishers, 2004.

[23] Daryl S.Reynolds, "Wireless communications," Course notes, WVU, Fall 2003.

[24] S.B.Weinstein and P.M.Ebert, "Data Transmission by Frequency-Division Multiplexing using the Discrete Fourier Transform," *IEEE Trans. Commun.*, vol. COM-19, pp. 628–634, Oct. 1971.

[25] Yi Gong and Khaled Ben Letaief, "An Efficient SpaceFrequency Coded OFDM System for Broadband Wireless Communications," *IEEE Trans. Commun.*, vol. 51, no. 11, pp. 2019–2029, Nov. 2003.